Red-Luminescent Biphosphine Stabilized '$Cu_{12}S_6$' Cluster Molecules

Xiao-Xun Yang,[ab] Ibrahim Issac,[bd] Sergej Lebedkin,[d] Michael Kühn,[c] Florian Weigend,[cd] Dieter Fenske,[abd] Olaf Fuhr,[ade] Andreas Eichhöfer,*[ade]

[a] Lehn Institute of Functional Materials, SunYat-Sen University, Guangzhou 510275, China

[b] Institut für Anorganische Chemie, Karlsruher Institut für Technologie (KIT), Campus Süd, Engesserstr. 15, 76131 Karlsruhe, Germany

[c] Institut für Physikalische Chemie, Abteilung für Theoretische Chemie, Karlsruher Institut für Technologie (KIT), Campus Süd, Fritz-Haber-Weg 2, 76131 Karlsruhe, Germany

[d] Institut für Nanotechnologie, Karlsruher Institut für Technologie (KIT), Campus Nord, Hermann-von-Helmholtz-Platz 1, 76344 Eggenstein-Leopoldshafen, Germany

Tel. 49-(0)721-608-26371

Fax: 49-(0)721-608-26368

e-mail: andreas.eichhoefer@kit.edu

[e] Karlsruhe Nano Micro Facility (KNMF)

Content

Experimental Section

Synthesis

Crystallography

Physical Measurements

Quantum chemical treatments

Table S1. Crystallographic data for $[Cu_{12}S_6(dpppt)_4]$ (**1**) and $[Cu_{12}S_6(dppo)_4]$ (**2**).

Table S2. Selected bond lengths and angles of $[Cu_{12}S_6(dpppt)_4]$ (**1**).

Table S3. Selected bond lengths and angles of $[Cu_{12}S_6(dppo)_4]$ (**2**).

Table S4. Lowest excitation energies for $[Cu_{12}S_6(dpppt)_4]$ (**1**) and $[Cu_{12}S_6(dppo)_4]$ (**2**) obtained at different levels of theory.

Table S5. Lowest 60 singlet and triplet transitions for $[Cu_{12}S_6(dpppt)_4]$ (**1**) and $[Cu_{12}S_6(dppo)_4]$ (**2**) at level B3LYP/def2-SV(P) (raw data for figure S10).

Figure S1. Measured (black) and simulated (grey) X–ray powder pattern for $[Cu_{12}S_6(dpppt)_4]$(**1**) as a suspension of crystals in toluene.

Figure S2. X–ray powder pattern for $[Cu_{12}S_6(dpppt)_4]$ (**1**) as a dried crystalline powder.

Figure S3. Measured (black) and simulated (grey) X–ray powder pattern for $[Cu_{12}S_6(dppo)_4]$ (**2**) as a suspension of crystals in toluene.

Figure S4. X–ray powder pattern of $[Cu_{12}S_6(dppo)_4]$ (**2**) as a dried crystalline powder.

Figure S5. Emission decay traces under 337 nm pulse excitation for $[Cu_{12}S_6(dpppt)_4]$ (**1**) and $[Cu_{12}S_6(dppo)_4]$ (**2**) as a suspension of microcrystals in toluene.

Figure S6. Steady-state photoluminescence excitation and emission spectra for $[Cu_{12}S_6(dpppt)_4]$ (**1**) and $[Cu_{12}S_6(dppo)_4]$ (**2**) as dried crystalline powders.

Figure S7. Photoluminescence decay traces for $[Cu_{12}S_6(dpppt)_4]$ (**1**) and $[Cu_{12}S_6(dppo)_4]$(**2**) as dried crystalline powders.

Figure S8. UV-Vis spectra of $[Cu_{12}S_6(dpppt)_4]$ (**1**) as a mull in nujol and as a solution in thf.

Figure S9. UV-Vis spectra of $[Cu_{12}S_6(dppo)_4]$ (**2**) as a mull in nujol and as a solution in thf.

Figure S10. PLE and PL spectra of $[Cu_{12}S_6(dpppt)_4]$ (**1**) in thf.

Figure S11. PLE and PL spectra of $[Cu_{12}S_6(dppo)_4]$ (**2**) in thf.

Figure S12. Comparison of the calculated excitation spectra for $[Cu_{12}S_6(dpppt)_4]$ (**1**) and $[Cu_{12}S_6(dppo)_4]$ (**2**) with the experimental spectra as a mull in nujol and as a solution in thf.

Figure S13. Calculated singlet and triplet excitation spectra of $[Cu_{12}S_6(dpppt)_4]$ (**1**) and $[Cu_{12}S_6(dppo)_4]$ (**2**).

Figure S14. a) Comparison of the molecular structures of $[Cu_{12}S_6(dpppt)_4]$ (**1**) as obtained from single crystal XRD and as optimized with DFT(BP86/def2-SV(P) and b) corresponding calculated electronic excitation spectra at level BP86/def2-SV(P).

Figure S15. a) Comparison of the molecular structures of $[Cu_{12}S_6(dppo)_4]$ (**2**) as obtained from single crystal XRD and as optimized with DFT(BP86/def2-SV(P) and b) corresponding calculated electronic excitation spectra at level BP86/def2-SV(P).

Figure S16. Comparison of calculated electronic singlet (black) and triplet (red and blue) excitation spectra of a) $[Cu_{12}S_6(dpppt)_4]$ (**1**) and b) $[Cu_{12}S_6(dppo)_4]$ (**2**) at level BP86/def2-SV(P)

Experimental Section

Synthesis

Standard Schlenk techniques were employed throughout the syntheses using a double manifold vacuum line with high purity dry nitrogen (99.9994 %) and a MBraun Glovebox with high purity dry argon (99.9990 %). The solvent Et_2O (diethylether) and toluene were dried over sodium-benzophenone, and distilled under nitrogen. $CuO(CO)CH_3$ [1] and $S(SiMe_3)_2$ [2] were prepared according to standard literature procedures. dpppt (bis(diphenylphosphino)pentane) was used as received from Aldrich.

Synthesis of dppo: 1,8-bis(diphenylphosphino)octane

Potassium (0.2 mol, 7.82 g) was suspended in 100 mL of thf in a 1L flask and refluxed. Then Ph_2PCl (18.1 mL, 0.1 mmol) diluted with 25 mL of thf was added dropwise to the refluxing solution. Refluxing and stirring was continued after the addition till all potassium disappeared to give a bright orange reaction mixture. Then $C_8H_{16}Cl_2$ (0.05 mol, 9.16 g) diluted in 150 mL of thf were added dropwise to the stirred solution at *rt*. After addition the reaction mixture was refluxed for additional 2 hours till the orange colour had disappeared completely and the suspension was almost white. Then 400 ml of degassed water were added carefully via the dropping funnel at *rt*. The two phases were separated after 1 additional hour of stirring and the water phase was washed two times with 50 ml of thf. After removal of one half of the solvent from the collected organic phases the product started to crystallize. By consecutive filtration and further concentration one can obtain 20 g (84 %) of dppo as a white crystalline material.

$C_{32}H_{36}P_2$ (482.59): calcd. C 79.6 H 7.5 found C 80.1 H 7.8 %

^{1}H (500 MHz, C_6D_6): 7.5 (t, 8H, *ortho*-C*H*), 7.1 (m, 12H, *meta*,*para*-C*H*); 2.0 (m, 4H, P-C$^1H_2$), 1.4 (m, 4H, -C$^2H_2$), 1.3 (m, 4H, C$^3H_2$), 1.07 (m, 4H, -C$^4H_2$)

^{31}P (500 MHz, C_6D_6): –16.4 ppm

$[Cu_{12}S_6(dpppt)_4]$ (**1**): Dpppt (0.45 g, 1.02mmol) and $CuO(CO)CH_3$ (0.125 g, 1.02 mmol) were dissolved in 30 mL of toluene. $S(SiMe_3)_2$ (0.11 mL, 0.51mmol) was then added at −40 °C to yield a clear colorless solution. Then, after warming up to +2 °C overnight in a fridge orange-red crystals of **1** appeared. After three days they were collected and washed two times with 10 mL of toluene and one time with 10 ml of Et_2O to give a final yield of 0.145 g (62.8 %).

$C_{112}H_{120}Cu_{12}P_8S_6$ (2716.9): calcd. C 51.3, H 4.5, S 7.1 found C 52.0, H 4.3, S 6.8 %.

$[Cu_{12}S_6(dppo)_4]$ (**2**): Dppo (0.244 g, 0.5 mmol) and $CuO(CO)CH_3$ (0.062 g, 0.5 mmol) were dissolved in 15 mL toluene. $S(SiMe_3)_2$ (0.053 mL, 0.25 mmol) was then added at 0 ^oC to yield a clear red solution. Then, after warming up to +2 ^oC overnight in a fridge red crystals of **2** appeared. After one week they were collected and washed with toluene to give a final yield of 0.064 mg (52.1 %).

$C_{128}H_{144}P_8S_6Cu_{12}$ (2885.25): C 53.30; H 5.03; S 6.67 found: C 53.56; H 5.08; S 6.38 %.

Crystallography

Crystals suitable for single crystal X-ray diffraction were selected in perfluoroalkylether oil and mounted to the diffractometer equipped with an Oxford Cryosystem. Single-crystal X-ray diffraction data of **1** were collected using graphite-monochromatised MoKα radiation (λ = 0.71073 Å) on a STOE IPDS II (Imaging Plate Diffraction System). Single-crystal X-ray diffraction data of **2** were collected using graphite-monochromatised MoKα radiation (λ = 0.71073 Å) on a STOE STADI Vari (Pilatus Hybrid Pixel Detector). Raw intensity data were collected and treated with the STOE X-Area software Version 1.64. Interframe Scaling of the STADI Vari dataset was done with the implemented program LANA. Data were corrected for Lorentz and polarisation effects.

Based on a crystal description a numerical absorption correction was applied for **1** and **2.**[3] The structures were solved with the direct methods program SHELXS of the SHELXTL PC suite programs,[4] and were refined with the use of the full-matrix least-squares program SHELXL. Molecular diagrams were prepared using Diamond.[5]

In **1** and **2** all Cu, S, P and C atoms were refined with anisotropic displacement parameters whilst H atoms were computed and refined, using a riding model, with an isotropic temperature factor equal to 1.2 the equivalent temperature factor of the atom which they are linked to. In **1** and **2** partially disordered solvent toluene molecules were refined with isotropic displacement parameters for the C atoms. Due to the disorder C–C distances and C–C–C angles partially differ from the expected ideal values of 139.5 pm and 120 °. Additional lattice toluene molecules were identified within the structure of **1**, but could not be adequately refined. The data were therefore corrected for these using the SQUEEZE option within the PLATON [6] program package finding a total of 346 electrons (~4 toluene) in an additional potential solvent accessible area of 1155 $Å^3$.

CCDC-994711 (**1**) and 994712 (**2**) contain the supplementary crystallographic data for this paper. These data can be obtained free of charge at www.ccdc.cam.ac.uk/conts/retrieving.html (or from the Cambridge Crystallographic Data Centre, 12 Union Road, CambridgeCB2 1EZ, UK; fax: (internat.) +44-1223/336-033; Email:deposit@ccdc.cam.ac.uk).

X-ray powder diffraction patterns (XRD) for **1** and **2** (suspension of crystals in toluene) were measured on a STOE STADI P diffractometer (Cu-$K_{\alpha 1}$ radiation, Germanium monochromator, Debye-Scherrer geometry, Mythen 1K detector) in sealed glass capillaries. The theoretical powder diffraction pattern were calculated on the basis of the atom coordinates obtained from single crystal X-ray analysis by using the program package STOE WinXPOW.[7]

Physical Measurements

C, H, S elemental analyses were performed on an `Elementarvario Micro cube´ instrument.

General Comments: ^{1}H-NMR, ^{13}C-NMR and ^{31}P-NMR spectra were recorded on a Bruker 500 MHz spectrometer. Chemical shifts are reported in ppm and referenced to tetramethylsilane and benzene (proton) and external 85% phosphoric acid (phosphorus)

UV-Vis solid state absorption spectra were measured on a Perkin Elmer Lambda 900 spectrophotometer in transmission as micron-sized crystalline powders between quartz plates in front of a Labsphere integrating sphere.

Photoluminescence (PL) measurements were performed on a Horiba JobinYvon Fluorolog-3 spectrometer. The emission spectra were corrected for the wavelength-dependent response of the spectrometer and detector (in relative photon flux units). Emission decay traces were recorded by connecting the detector (photomultiplier) to an oscilloscope and using a N_2–laser for pulsed excitation at 337 nm (~2 ns, ~5 μJ per pulse). PL quantum yields, φ_{PL} ,were measured at ambient temperature using a 10 cm integrating sphere out of optical PTFE with low auto-luminescence (Berghof GmbH), which was installed in the sample chamber of the

Fluorolog-3. Crystalline powders of **1** and **2** were placed into 0.2 mm glass tubes and excited at 500 nm. Their emission, relative absorption at the excitation wavelength and, correspondingly, φ_{PL}, were referenced to those of the Rhodamine 110 laser dye dissolved in methanol (also placed in a glass tube, inserted into the integrating sphere and excited at 500 nm), according to a procedure described elsewhere.[8] The fluorescence quantum yield of the laser dye was taken as 0.92.[9] The accuracy of the determination of φ_{PL} values was estimated to be ±10%.

Photoluminescence (PL) measurements in solution were recorded in quartz cuvettes which were filled under nitrogen inert gas atmosphere by using a Varian Cary Eclipse spectrometer.

Quantum Chemical Treatments

All calculations were carried out with TURBOMOLE.[10] The spectra in the paper were obtained at level B3-LYP[11]/def2-SV(P)[12] for the structure parameters of the X-ray structure analysis using time-dependent density functional theory, TDDFT. The electronic spectrum and the (non-relaxed) transition densities for a group of transitions forming a peak were visualized at essentially no extra computational effort using the Python script PANAMA (**P**eak **ANA**lyzing **MA**chine), which was written in occasion of this work and will be available with TURBOMOLE V 6.7. It is done as follows.

The electronic spectrum is simulated by taking excitation energies and corresponding oscillator strengths from the TDDFT output file. The (delta function-shaped) peaks are broadened using Gaussian functions with adjustable FWHM (full width at half maximum), chosen to 0.1 eV in the present work.

For the visualization of the (non-relaxed) transition densities, the normalized weights/contributions of a one-electron transition from an occupied orbital *i* to a virtual orbital *a* for the *n*th excitation, $\boldsymbol{w_{ia,n}}$, as well as the corresponding oscillator strengths $\boldsymbol{f_{0n}}$ are taken from the TDDFT output file. The total contributions, weighted with the oscillator strengths,

for a peak in the spectrum, that is often composed of multiple excitations ($\boldsymbol{n = M_1, M_1 + 1, \ldots, M_2}$), is given as

$$W_{ia}^{M_1,M_2} = \sum_{n=M_1}^{M_2} w_{ia,n} f_{0n}$$

The resulting change in the occupation number of occupied orbital *i* is then

$$\Delta N_i^{M_1,M_2} = -\frac{2}{C^{M_1,M_2}} \sum_a W_{ia}^{M_1,M_2}$$

and of the virtual orbital *a*

$$\Delta N_a^{M_1,M_2} = \frac{2}{C^{M_1,M_2}} \sum_i W_{ia}^{M_1,M_2}$$

The factor of 2 arises when closed-shell systems are considered, and $C^{M_1,M_2} = \sum_{ia} W_{ia}^{M_1,M_2}$ is the normalization constant. We note in passing that in the TDDFT output file only dominant $\boldsymbol{w_{ia,n}}$ are listed accounting for at least 90% of all contributing one-electron transitions.

After writing $\boldsymbol{\Delta N_i^{M_1,M_2}}$ and $\boldsymbol{\Delta N_a^{M_1,M_2}}$ to the TURBOMOLE input file as (pseudo-) occupation numbers, a Mulliken population analysis may be performed along with the calculation of the (total) electronic densities arising from $\boldsymbol{\Delta N_i^{M_1,M_2}}$ and $\boldsymbol{\Delta N_a^{M_1,M_2}}$ on Cartesian grid, written to a file of selectable output format, e.g. '.plt' for gOpenMol.[13]

The spectra in the paper are calculated with def2-SV(P) bases for the X-ray structure, but results do not change qualitatively when either employing larger bases (def2-TZVP)[12] or the optimized structure parameters, see Figures S14 – S16. For the non-hybrid functional BP86[14] a red-shift by ca. 0.9 compared to B3-LYP is observed.

Table S1. Crystallographic data for $[Cu_{12}S_6(dpppt)_4]$ (**1**) and $[Cu_{12}S_6(dppo)_4]$ (**2**).

			1 · 2 $C_6H_5CH_3$	**2** · 3.5 $C_6H_5CH_3$
sum formula[a]			$C_{130}H_{136}Cu_{12}S_6P_8$	$C_{152.5}H_{172}Cu_{12}S_6P_8$
fw[g/mol]			2900.99	3207.50
crystal system			tetragonal	triclinic
space group			$P4_2/ncm$	$P\bar{1}$
Cell	*a*	[pm]	2608.1(4)	1780.3(4)
	b			1852.2(4)
	c		1931.3(4)	2371.3(5)
	α	[°]		83.46(3)
	β			80.88(3))
	γ			71.93(3)
V [10^6pm^3]			13137(4)	7322(3)
Z			4	2
T [K]			180(2)	150(2)
d_c [g cm^{-3}]			1.467	1.455
$\mu(\lambda)$ [mm^{-1}]			2.138	1.925
F[000]			5920	3302
$2\theta_{max}$ [°]			54	55
meas reflns			52835	117021
unique reflns			7189	34384
R_{int}			0.0528	0.0514
reflns with $I > 2\sigma(I)$.			5578	23989
refined params			348	1509
$R1(I > 2\sigma(I))$[b]			0.0326	0.0434
*wR*2(all data)[c]			0.0859	0.1153

[a] no H atoms where calculated on disordered toluene molecules

[b] $R1 = \Sigma||F_o| - |F_c||/\Sigma|F_o|$.

[c] $wR2 = \{\Sigma[w(F_o^2 - F_c^2)^2] / \Sigma[w(F_o^2)^2]\}^{1/2}$

Table S2. Selected bond lengths [pm] and angles [°] of $[Cu_{12}S_6(dpppt)_4]$ (**1**).

Cu(1)-S(1)	226.75(6)
Cu(1)-P(1)	227.66(8)
Cu(1)-S(3)#1	236.77(6)
Cu(1)-Cu(3)	263.31(5)
Cu(1)-Cu(4)#1	265.77(6)
Cu(1)-Cu(2)#2	281.88(6)
Cu(1)-Cu(2)	289.42(6)
Cu(2)-S(1)	226.14(6)
Cu(2)-P(2)	228.77(8)
Cu(2)-S(2)	237.82(6)
Cu(2)-Cu(4)	262.59(5)
Cu(2)-Cu(3)	268.06(5)
Cu(2)-Cu(1)#2	281.88(6)
Cu(3)-S(2)	215.45(11)
Cu(3)-S(3)#1	216.78(11)
Cu(3)-Cu(1)#3	263.32(5)
Cu(3)-Cu(2)#3	268.07(5)
Cu(3)-Cu(4)	294.12(9)
Cu(3)-Cu(4)#1	294.15(8)
Cu(4)-S(3)	215.95(11)
Cu(4)-S(2)	216.89(11)
Cu(4)-Cu(2)#3	262.59(5)
Cu(4)-Cu(1)#2	265.76(6)
Cu(4)-Cu(1)#1	265.76(6)
Cu(4)-Cu(3)#1	294.14(8)
S(1)-Cu(2)#2	226.14(6)
S(1)-Cu(1)#2	226.75(6)
S(2)-Cu(2)#3	237.82(6)
S(3)-Cu(3)#1	216.78(11)
S(3)-Cu(1)#2	236.77(6)
S(3)-Cu(1)#1	236.77(6)
S(1)-Cu(1)-P(1)	119.13(3)
S(1)-Cu(1)-S(3)#1	142.94(3)
P(1)-Cu(1)-S(3)#1	97.76(3)
S(1)-Cu(1)-Cu(3)	100.12(2)
P(1)-Cu(1)-Cu(3)	124.43(3)
S(3)#1-Cu(1)-Cu(3)	51.04(3)
S(1)-Cu(1)-Cu(4)#1	100.57(2)
P(1)-Cu(1)-Cu(4)#1	131.97(2)
S(3)#1-Cu(1)-Cu(4)#1	50.50(3)
Cu(3)-Cu(1)-Cu(4)#1	67.554(15)
S(1)-Cu(1)-Cu(2)#2	51.412(14)
P(1)-Cu(1)-Cu(2)#2	130.63(2)
S(3)#1-Cu(1)-Cu(2)#2	107.66(3)
Cu(3)-Cu(1)-Cu(2)#2	104.236(17)
Cu(4)#1-Cu(1)-Cu(2)#2	57.213(13)
S(1)-Cu(1)-Cu(2)	50.185(15)
P(1)-Cu(1)-Cu(2)	121.11(3)
S(3)#1-Cu(1)-Cu(2)	108.80(3)
Cu(3)-Cu(1)-Cu(2)	57.791(12)
Cu(4)#1-Cu(1)-Cu(2)	104.561(16)
Cu(2)#2-Cu(1)-Cu(2)	89.956(18)
S(1)-Cu(2)-P(2)	123.41(3)
S(1)-Cu(2)-S(2)	142.47(3)
P(2)-Cu(2)-S(2)	94.12(3)

S(1)-Cu(2)-Cu(4)	101.69(2)
P(2)-Cu(2)-Cu(4)	121.80(3)
S(2)-Cu(2)-Cu(4)	51.08(3)
S(1)-Cu(2)-Cu(3)	98.89(2)
P(2)-Cu(2)-Cu(3)	129.05(3)
S(2)-Cu(2)-Cu(3)	49.98(2)
Cu(4)-Cu(2)-Cu(3)	67.310(19)
S(1)-Cu(2)-Cu(1)#2	51.606(14)
P(2)-Cu(2)-Cu(1)#2	124.03(2)
S(2)-Cu(2)-Cu(1)#2	109.38(3)
Cu(4)-Cu(2)-Cu(1)#2	58.304(14)
Cu(3)-Cu(2)-Cu(1)#2	103.676(17)
S(1)-Cu(2)-Cu(1)	50.372(13)
P(2)-Cu(2)-Cu(1)	131.87(2)
S(2)-Cu(2)-Cu(1)	106.06(3)
Cu(4)-Cu(2)-Cu(1)	104.438(18)
Cu(3)-Cu(2)-Cu(1)	56.213(14)
Cu(1)#2-Cu(2)-Cu(1)	90.043(18)
S(2)-Cu(3)-S(3)#1	173.99(5)
S(2)-Cu(3)-Cu(1)	123.522(13)
S(3)#1-Cu(3)-Cu(1)	58.136(14)
S(2)-Cu(3)-Cu(1)#3	123.522(13)
S(3)#1-Cu(3)-Cu(1)#3	58.135(14)
Cu(1)-Cu(3)-Cu(1)#3	107.89(2)
S(2)-Cu(3)-Cu(2)	57.702(15)
S(3)#1-Cu(3)-Cu(2)	124.095(15)
Cu(1)-Cu(3)-Cu(2)	65.997(13)
Cu(1)#3-Cu(3)-Cu(2)	152.07(2)
S(2)-Cu(3)-Cu(2)#3	57.702(15)
S(3)#1-Cu(3)-Cu(2)#3	124.094(15)
Cu(1)-Cu(3)-Cu(2)#3	152.07(2)
Cu(1)#3-Cu(3)-Cu(2)#3	65.996(13)
Cu(2)-Cu(3)-Cu(2)#3	105.88(2)
S(2)-Cu(3)-Cu(4)	47.34(3)
S(3)#1-Cu(3)-Cu(4)	138.67(4)
Cu(1)-Cu(3)-Cu(4)	102.975(15)
Cu(1)#3-Cu(3)-Cu(4)	102.975(16)
Cu(2)-Cu(3)-Cu(4)	55.457(13)
Cu(2)#3-Cu(3)-Cu(4)	55.457(13)
S(2)-Cu(3)-Cu(4)#1	138.95(3)
S(3)#1-Cu(3)-Cu(4)#1	47.06(3)
Cu(1)-Cu(3)-Cu(4)#1	56.621(12)
Cu(1)#3-Cu(3)-Cu(4)#1	56.620(12)
Cu(2)-Cu(3)-Cu(4)#1	102.706(15)
Cu(2)#3-Cu(3)-Cu(4)#1	102.706(15)
Cu(4)-Cu(3)-Cu(4)#1	91.612(19)
S(3)-Cu(4)-S(2)	177.39(4)
S(3)-Cu(4)-Cu(2)	122.195(15)
S(2)-Cu(4)-Cu(2)	58.546(14)
S(3)-Cu(4)-Cu(2)#3	122.194(15)
S(2)-Cu(4)-Cu(2)#3	58.547(14)
Cu(2)-Cu(4)-Cu(2)#3	109.11(2)
S(3)-Cu(4)-Cu(1)#2	57.778(14)
S(2)-Cu(4)-Cu(1)#2	123.028(14)
Cu(2)-Cu(4)-Cu(1)#2	64.482(11)
Cu(2)#3-Cu(4)-Cu(1)#2	150.96(2)
S(3)-Cu(4)-Cu(1)#1	57.778(14)
S(2)-Cu(4)-Cu(1)#1	123.028(14)
Cu(2)-Cu(4)-Cu(1)#1	150.96(2)
Cu(2)#3-Cu(4)-Cu(1)#1	64.481(11)

Cu(1)#2-Cu(4)-Cu(1)#1	106.45(2)
S(3)-Cu(4)-Cu(3)	135.68(3)
S(2)-Cu(4)-Cu(3)	46.93(3)
Cu(2)-Cu(4)-Cu(3)	57.232(12)
Cu(2)#3-Cu(4)-Cu(3)	57.234(12)
Cu(1)#2-Cu(4)-Cu(3)	101.030(14)
Cu(1)#1-Cu(4)-Cu(3)	101.030(14)
S(3)-Cu(4)-Cu(3)#1	47.30(3)
S(2)-Cu(4)-Cu(3)#1	135.31(3)
Cu(2)-Cu(4)-Cu(3)#1	101.130(15)
Cu(2)#3-Cu(4)-Cu(3)#1	101.129(15)
Cu(1)#2-Cu(4)-Cu(3)#1	55.829(12)
Cu(1)#1-Cu(4)-Cu(3)#1	55.829(12)
Cu(3)-Cu(4)-Cu(3)#1	88.387(19)
Cu(2)-S(1)-Cu(2)#2	126.49(4)
Cu(2)-S(1)-Cu(1)#2	76.98(2)
Cu(2)#2-S(1)-Cu(1)#2	79.44(2)
Cu(2)-S(1)-Cu(1)	79.44(2)
Cu(2)#2-S(1)-Cu(1)	76.98(2)
Cu(1)#2-S(1)-Cu(1)	126.05(4)
Cu(3)-S(2)-Cu(4)	85.73(4)
Cu(3)-S(2)-Cu(2)	72.32(2)
Cu(4)-S(2)-Cu(2)	70.38(2)
Cu(3)-S(2)-Cu(2)#3	72.32(2)
Cu(4)-S(2)-Cu(2)#3	70.38(2)
Cu(2)-S(2)-Cu(2)#3	128.19(4)
Cu(4)-S(3)-Cu(3)#1	85.64(4)
Cu(4)-S(3)-Cu(1)#2	71.72(2)
Cu(3)#1-S(3)-Cu(1)#2	70.82(2)
Cu(4)-S(3)-Cu(1)#1	71.72(2)
Cu(3)#1-S(3)-Cu(1)#1	70.82(2)
Cu(1)#2-S(3)-Cu(1)#1	128.07(4)

Symmetry transformations used to generate equivalent atoms:
#1 -x+1,-y,-z #2 y+1/2,x-1/2,-z #3 -y+1/2,-x+1/2,z
#4 -x+1/2,-y+1/2,z

Table S3. Selected bond lengths [pm] and angles [°] of $[Cu_{12}S_6(dppo)_4]$ (**2**).

Cu(1)-S(1)	226.61(10)
Cu(1)-P(1)	229.04(11)
Cu(1)-S(2)	236.79(10)
Cu(1)-Cu(8)	260.45(10)
Cu(1)-Cu(5)	268.68(11)
Cu(1)-Cu(2)	285.45(11)
Cu(1)-Cu(4)	289.51(12)
Cu(2)-S(1)	227.01(13)
Cu(2)-P(2)	229.14(12)
Cu(2)-S(3)	237.22(12)
Cu(2)-Cu(5)	259.33(8)
Cu(2)-Cu(6)	269.81(10)
Cu(2)-Cu(3)	286.60(11)
Cu(3)-S(1)	226.07(9)
Cu(3)-P(3)	228.68(10)
Cu(3)-S(4)	235.69(12)
Cu(3)-Cu(6)	258.10(9)
Cu(3)-Cu(7)	272.53(9)
Cu(3)-Cu(4)	298.06(12)
Cu(4)-S(1)	227.08(11)
Cu(4)-P(4)	230.30(12)
Cu(4)-S(5)	236.37(11)
Cu(4)-Cu(7)	260.14(10)
Cu(4)-Cu(8)	270.72(8)
Cu(5)-S(3)	216.95(12)
Cu(5)-S(2)	217.37(11)
Cu(5)-Cu(9)	257.13(8)
Cu(5)-Cu(10)	268.82(10)
Cu(5)-Cu(6)	294.35(8)
Cu(5)-Cu(8)	296.30(13)
Cu(6)-S(3)	217.42(12)
Cu(6)-S(4)	217.45(12)
Cu(6)-Cu(10)	259.30(8)
Cu(6)-Cu(11)	270.13(10)
Cu(6)-Cu(7)	293.70(13)
Cu(7)-S(5)	217.58(12)
Cu(7)-S(4)	217.96(11)
Cu(7)-Cu(11)	259.66(11)
Cu(7)-Cu(12)	274.30(8)
Cu(7)-Cu(8)	293.84(8)
Cu(8)-S(2)	217.44(11)
Cu(8)-S(5)	217.88(12)
Cu(8)-Cu(12)	258.21(10)
Cu(8)-Cu(9)	272.98(9)
Cu(9)-S(6)	226.80(9)
Cu(9)-P(5)	227.68(10)
Cu(9)-S(2)	236.75(12)
Cu(9)-Cu(10)	281.10(11)
Cu(9)-Cu(12)	291.59(12)
Cu(10)-S(6)	225.19(11)
Cu(10)-P(6)	228.29(13)
Cu(10)-S(3)	236.73(11)
Cu(10)-Cu(11)	290.69(12)
Cu(11)-S(6)	225.96(10)
Cu(11)-P(7)	228.80(11)
Cu(11)-S(4)	236.38(11)
Cu(11)-Cu(12)	290.13(11)

Cu(12)-S(6)	226.59(13)
Cu(12)-P(8)	228.47(11)
Cu(12)-S(5)	237.06(12)
S(1)-Cu(1)-P(1)	117.70(4)
S(1)-Cu(1)-S(2)	141.61(4)
P(1)-Cu(1)-S(2)	100.18(4)
S(1)-Cu(1)-Cu(8)	100.02(3)
P(1)-Cu(1)-Cu(8)	120.33(4)
S(2)-Cu(1)-Cu(8)	51.59(3)
S(1)-Cu(1)-Cu(5)	98.27(3)
P(1)-Cu(1)-Cu(5)	138.56(4)
S(2)-Cu(1)-Cu(5)	50.46(3)
Cu(8)-Cu(1)-Cu(5)	68.09(3)
S(1)-Cu(1)-Cu(2)	51.07(3)
P(1)-Cu(1)-Cu(2)	134.84(4)
S(2)-Cu(1)-Cu(2)	106.03(4)
Cu(8)-Cu(1)-Cu(2)	104.76(3)
Cu(5)-Cu(1)-Cu(2)	55.71(3)
S(1)-Cu(1)-Cu(4)	50.42(3)
P(1)-Cu(1)-Cu(4)	113.32(4)
S(2)-Cu(1)-Cu(4)	110.28(3)
Cu(8)-Cu(1)-Cu(4)	58.69(3)
Cu(5)-Cu(1)-Cu(4)	105.17(3)
Cu(2)-Cu(1)-Cu(4)	91.24(3)
S(1)-Cu(2)-P(2)	117.56(5)
S(1)-Cu(2)-S(3)	141.03(4)
P(2)-Cu(2)-S(3)	100.77(5)
S(1)-Cu(2)-Cu(5)	100.90(3)
P(2)-Cu(2)-Cu(5)	117.28(3)
S(3)-Cu(2)-Cu(5)	51.58(3)
S(1)-Cu(2)-Cu(6)	96.68(4)
P(2)-Cu(2)-Cu(6)	141.94(4)
S(3)-Cu(2)-Cu(6)	50.28(3)
Cu(5)-Cu(2)-Cu(6)	67.56(3)
S(1)-Cu(2)-Cu(1)	50.94(3)
P(2)-Cu(2)-Cu(1)	110.86(3)
S(3)-Cu(2)-Cu(1)	110.44(4)
Cu(5)-Cu(2)-Cu(1)	58.87(2)
Cu(6)-Cu(2)-Cu(1)	103.37(3)
S(1)-Cu(2)-Cu(3)	50.61(3)
P(2)-Cu(2)-Cu(3)	137.19(3)
S(3)-Cu(2)-Cu(3)	105.12(3)
Cu(5)-Cu(2)-Cu(3)	105.52(3)
Cu(6)-Cu(2)-Cu(3)	55.17(3)
Cu(1)-Cu(2)-Cu(3)	91.26(3)
S(1)-Cu(3)-P(3)	118.07(4)
S(1)-Cu(3)-S(4)	139.99(3)
P(3)-Cu(3)-S(4)	101.84(4)
S(1)-Cu(3)-Cu(6)	100.30(4)
P(3)-Cu(3)-Cu(6)	121.75(4)
S(4)-Cu(3)-Cu(6)	52.01(3)
S(1)-Cu(3)-Cu(7)	95.20(4)
P(3)-Cu(3)-Cu(7)	140.36(3)
S(4)-Cu(3)-Cu(7)	50.15(3)
Cu(6)-Cu(3)-Cu(7)	67.15(3)
S(1)-Cu(3)-Cu(2)	50.91(3)
P(3)-Cu(3)-Cu(2)	114.38(3)
S(4)-Cu(3)-Cu(2)	111.11(3)
Cu(6)-Cu(3)-Cu(2)	59.11(3)

Cu(7)-Cu(3)-Cu(2)	103.05(3)
S(1)-Cu(3)-Cu(4)	49.02(3)
P(3)-Cu(3)-Cu(4)	135.20(3)
S(4)-Cu(3)-Cu(4)	103.96(3)
Cu(6)-Cu(3)-Cu(4)	102.98(3)
Cu(7)-Cu(3)-Cu(4)	54.02(2)
Cu(2)-Cu(3)-Cu(4)	89.30(3)
S(1)-Cu(4)-P(4)	116.28(5)
S(1)-Cu(4)-S(5)	140.14(4)
P(4)-Cu(4)-S(5)	103.20(4)
S(1)-Cu(4)-Cu(7)	98.42(4)
P(4)-Cu(4)-Cu(7)	123.82(4)
S(5)-Cu(4)-Cu(7)	51.71(3)
S(1)-Cu(4)-Cu(8)	96.95(4)
P(4)-Cu(4)-Cu(8)	140.33(3)
S(5)-Cu(4)-Cu(8)	50.34(3)
Cu(7)-Cu(4)-Cu(8)	67.18(3)
S(1)-Cu(4)-Cu(1)	50.28(3)
P(4)-Cu(4)-Cu(1)	133.17(3)
S(5)-Cu(4)-Cu(1)	105.51(3)
Cu(7)-Cu(4)-Cu(1)	103.00(3)
Cu(8)-Cu(4)-Cu(1)	55.28(2)
S(1)-Cu(4)-Cu(3)	48.72(3)
P(4)-Cu(4)-Cu(3)	115.59(4)
S(5)-Cu(4)-Cu(3)	109.68(3)
Cu(7)-Cu(4)-Cu(3)	57.97(3)
Cu(8)-Cu(4)-Cu(3)	102.36(3)
Cu(1)-Cu(4)-Cu(3)	88.20(3)
S(3)-Cu(5)-S(2)	176.37(4)
S(3)-Cu(5)-Cu(9)	121.42(4)
S(2)-Cu(5)-Cu(9)	59.15(3)
S(3)-Cu(5)-Cu(2)	58.95(3)
S(2)-Cu(5)-Cu(2)	122.37(4)
Cu(9)-Cu(5)-Cu(2)	154.12(2)
S(3)-Cu(5)-Cu(1)	124.36(4)
S(2)-Cu(5)-Cu(1)	57.14(4)
Cu(9)-Cu(5)-Cu(1)	107.89(3)
Cu(2)-Cu(5)-Cu(1)	65.42(3)
S(3)-Cu(5)-Cu(10)	57.14(3)
S(2)-Cu(5)-Cu(10)	123.70(4)
Cu(9)-Cu(5)-Cu(10)	64.57(3)
Cu(2)-Cu(5)-Cu(10)	107.22(3)
Cu(1)-Cu(5)-Cu(10)	148.63(3)
S(3)-Cu(5)-Cu(6)	47.41(3)
S(2)-Cu(5)-Cu(6)	136.21(3)
Cu(9)-Cu(5)-Cu(6)	101.84(3)
Cu(2)-Cu(5)-Cu(6)	57.91(3)
Cu(1)-Cu(5)-Cu(6)	101.32(3)
Cu(10)-Cu(5)-Cu(6)	54.60(2)
S(3)-Cu(5)-Cu(8)	136.56(3)
S(2)-Cu(5)-Cu(8)	47.05(3)
Cu(9)-Cu(5)-Cu(8)	58.60(2)
Cu(2)-Cu(5)-Cu(8)	102.07(3)
Cu(1)-Cu(5)-Cu(8)	54.64(3)
Cu(10)-Cu(5)-Cu(8)	101.04(4)
Cu(6)-Cu(5)-Cu(8)	89.16(3)
S(3)-Cu(6)-S(4)	174.32(4)
S(3)-Cu(6)-Cu(3)	122.31(4)
S(4)-Cu(6)-Cu(3)	58.68(3)
S(3)-Cu(6)-Cu(10)	58.77(3)

S(4)-Cu(6)-Cu(10)	123.06(3)
Cu(3)-Cu(6)-Cu(10)	155.68(2)
S(3)-Cu(6)-Cu(2)	57.06(3)
S(4)-Cu(6)-Cu(2)	124.39(4)
Cu(3)-Cu(6)-Cu(2)	65.72(3)
Cu(10)-Cu(6)-Cu(2)	106.94(3)
S(3)-Cu(6)-Cu(11)	125.34(4)
S(4)-Cu(6)-Cu(11)	56.77(3)
Cu(3)-Cu(6)-Cu(11)	107.37(4)
Cu(10)-Cu(6)-Cu(11)	66.57(3)
Cu(2)-Cu(6)-Cu(11)	149.87(3)
S(3)-Cu(6)-Cu(7)	138.01(3)
S(4)-Cu(6)-Cu(7)	47.66(3)
Cu(3)-Cu(6)-Cu(7)	58.77(3)
Cu(10)-Cu(6)-Cu(7)	103.00(3)
Cu(2)-Cu(6)-Cu(7)	101.88(4)
Cu(11)-Cu(6)-Cu(7)	54.65(3)
S(3)-Cu(6)-Cu(5)	47.27(3)
S(4)-Cu(6)-Cu(5)	138.40(3)
Cu(3)-Cu(6)-Cu(5)	103.67(3)
Cu(10)-Cu(6)-Cu(5)	57.68(3)
Cu(2)-Cu(6)-Cu(5)	54.52(2)
Cu(11)-Cu(6)-Cu(5)	102.88(3)
Cu(7)-Cu(6)-Cu(5)	90.74(4)
S(5)-Cu(7)-S(4)	175.00(4)
S(5)-Cu(7)-Cu(11)	121.61(4)
S(4)-Cu(7)-Cu(11)	58.55(4)
S(5)-Cu(7)-Cu(4)	58.50(4)
S(4)-Cu(7)-Cu(4)	123.81(4)
Cu(11)-Cu(7)-Cu(4)	155.12(3)
S(5)-Cu(7)-Cu(3)	126.50(3)
S(4)-Cu(7)-Cu(3)	56.12(3)
Cu(11)-Cu(7)-Cu(3)	106.22(4)
Cu(4)-Cu(7)-Cu(3)	68.00(3)
S(5)-Cu(7)-Cu(12)	56.21(3)
S(4)-Cu(7)-Cu(12)	124.30(4)
Cu(11)-Cu(7)-Cu(12)	65.76(3)
Cu(4)-Cu(7)-Cu(12)	106.16(3)
Cu(3)-Cu(7)-Cu(12)	149.31(2)
S(5)-Cu(7)-Cu(6)	137.36(3)
S(4)-Cu(7)-Cu(6)	47.51(3)
Cu(11)-Cu(7)-Cu(6)	58.05(3)
Cu(4)-Cu(7)-Cu(6)	103.66(4)
Cu(3)-Cu(7)-Cu(6)	54.08(2)
Cu(12)-Cu(7)-Cu(6)	101.57(2)
S(5)-Cu(7)-Cu(8)	47.61(3)
S(4)-Cu(7)-Cu(8)	137.26(3)
Cu(11)-Cu(7)-Cu(8)	102.18(3)
Cu(4)-Cu(7)-Cu(8)	58.13(2)
Cu(3)-Cu(7)-Cu(8)	103.01(3)
Cu(12)-Cu(7)-Cu(8)	53.93(2)
Cu(6)-Cu(7)-Cu(8)	89.76(3)
S(2)-Cu(8)-S(5)	175.11(4)
S(2)-Cu(8)-Cu(12)	122.45(4)
S(5)-Cu(8)-Cu(12)	59.00(3)
S(2)-Cu(8)-Cu(1)	58.58(3)
S(5)-Cu(8)-Cu(1)	122.50(4)
Cu(12)-Cu(8)-Cu(1)	154.61(3)
S(2)-Cu(8)-Cu(4)	124.59(3)
S(5)-Cu(8)-Cu(4)	56.63(3)

Cu(12)-Cu(8)-Cu(4)	107.78(3)
Cu(1)-Cu(8)-Cu(4)	66.02(3)
S(2)-Cu(8)-Cu(9)	56.37(3)
S(5)-Cu(8)-Cu(9)	125.49(4)
Cu(12)-Cu(8)-Cu(9)	66.52(3)
Cu(1)-Cu(8)-Cu(9)	105.67(4)
Cu(4)-Cu(8)-Cu(9)	149.72(2)
S(2)-Cu(8)-Cu(7)	137.36(3)
S(5)-Cu(8)-Cu(7)	47.52(3)
Cu(12)-Cu(8)-Cu(7)	59.17(2)
Cu(1)-Cu(8)-Cu(7)	101.77(3)
Cu(4)-Cu(8)-Cu(7)	54.69(3)
Cu(9)-Cu(8)-Cu(7)	102.36(3)
S(2)-Cu(8)-Cu(5)	47.03(3)
S(5)-Cu(8)-Cu(5)	137.85(3)
Cu(12)-Cu(8)-Cu(5)	103.27(4)
Cu(1)-Cu(8)-Cu(5)	57.28(3)
Cu(4)-Cu(8)-Cu(5)	102.84(3)
Cu(9)-Cu(8)-Cu(5)	53.51(3)
Cu(7)-Cu(8)-Cu(5)	90.33(3)
S(6)-Cu(9)-P(5)	116.78(4)
S(6)-Cu(9)-S(2)	140.86(3)
P(5)-Cu(9)-S(2)	102.30(4)
S(6)-Cu(9)-Cu(5)	101.67(4)
P(5)-Cu(9)-Cu(5)	121.22(4)
S(2)-Cu(9)-Cu(5)	52.02(3)
S(6)-Cu(9)-Cu(8)	96.11(4)
P(5)-Cu(9)-Cu(8)	140.37(3)
S(2)-Cu(9)-Cu(8)	49.88(3)
Cu(5)-Cu(9)-Cu(8)	67.89(3)
S(6)-Cu(9)-Cu(10)	51.29(3)
P(5)-Cu(9)-Cu(10)	113.61(4)
S(2)-Cu(9)-Cu(10)	111.73(3)
Cu(5)-Cu(9)-Cu(10)	59.73(2)
Cu(8)-Cu(9)-Cu(10)	103.96(3)
S(6)-Cu(9)-Cu(12)	49.94(3)
P(5)-Cu(9)-Cu(12)	133.84(3)
S(2)-Cu(9)-Cu(12)	103.88(4)
Cu(5)-Cu(9)-Cu(12)	104.86(3)
Cu(8)-Cu(9)-Cu(12)	54.31(3)
Cu(10)-Cu(9)-Cu(12)	90.74(3)
S(6)-Cu(10)-P(6)	118.33(5)
S(6)-Cu(10)-S(3)	142.04(4)
P(6)-Cu(10)-S(3)	99.26(4)
S(6)-Cu(10)-Cu(6)	100.13(4)
P(6)-Cu(10)-Cu(6)	121.05(3)
S(3)-Cu(10)-Cu(6)	51.75(3)
S(6)-Cu(10)-Cu(5)	98.63(4)
P(6)-Cu(10)-Cu(5)	137.12(4)
S(3)-Cu(10)-Cu(5)	50.33(3)
Cu(6)-Cu(10)-Cu(5)	67.72(3)
S(6)-Cu(10)-Cu(9)	51.80(3)
P(6)-Cu(10)-Cu(9)	133.77(3)
S(3)-Cu(10)-Cu(9)	105.82(3)
Cu(6)-Cu(10)-Cu(9)	104.93(3)
Cu(5)-Cu(10)-Cu(9)	55.70(3)
S(6)-Cu(10)-Cu(11)	50.00(3)
P(6)-Cu(10)-Cu(11)	115.85(3)
S(3)-Cu(10)-Cu(11)	110.25(3)
Cu(6)-Cu(10)-Cu(11)	58.50(2)

Cu(5)-Cu(10)-Cu(11)	104.18(3)
Cu(9)-Cu(10)-Cu(11)	91.03(3)
S(6)-Cu(11)-P(7)	116.70(4)
S(6)-Cu(11)-S(4)	141.36(4)
P(7)-Cu(11)-S(4)	101.59(4)
S(6)-Cu(11)-Cu(7)	100.82(3)
P(7)-Cu(11)-Cu(7)	120.01(4)
S(4)-Cu(11)-Cu(7)	51.87(3)
S(6)-Cu(11)-Cu(6)	96.81(3)
P(7)-Cu(11)-Cu(6)	141.36(3)
S(4)-Cu(11)-Cu(6)	50.31(3)
Cu(7)-Cu(11)-Cu(6)	67.30(3)
S(6)-Cu(11)-Cu(12)	50.22(3)
P(7)-Cu(11)-Cu(12)	112.45(4)
S(4)-Cu(11)-Cu(12)	111.42(3)
Cu(7)-Cu(11)-Cu(12)	59.55(3)
Cu(6)-Cu(11)-Cu(12)	103.53(2)
S(6)-Cu(11)-Cu(10)	49.77(3)
P(7)-Cu(11)-Cu(10)	136.26(4)
S(4)-Cu(11)-Cu(10)	105.04(3)
Cu(7)-Cu(11)-Cu(10)	103.73(3)
Cu(6)-Cu(11)-Cu(10)	54.93(3)
Cu(12)-Cu(11)-Cu(10)	89.15(3)
S(6)-Cu(12)-P(8)	116.88(4)
S(6)-Cu(12)-S(5)	140.61(4)
P(8)-Cu(12)-S(5)	102.43(5)
S(6)-Cu(12)-Cu(8)	100.40(4)
P(8)-Cu(12)-Cu(8)	123.09(4)
S(5)-Cu(12)-Cu(8)	51.98(3)
S(6)-Cu(12)-Cu(7)	96.43(3)
P(8)-Cu(12)-Cu(7)	139.78(3)
S(5)-Cu(12)-Cu(7)	49.71(3)
Cu(8)-Cu(12)-Cu(7)	66.90(3)
S(6)-Cu(12)-Cu(11)	50.03(3)
P(8)-Cu(12)-Cu(11)	133.26(3)
S(5)-Cu(12)-Cu(11)	104.14(4)
Cu(8)-Cu(12)-Cu(11)	103.56(3)
Cu(7)-Cu(12)-Cu(11)	54.69(2)
S(6)-Cu(12)-Cu(9)	50.00(3)
P(8)-Cu(12)-Cu(9)	115.78(4)
S(5)-Cu(12)-Cu(9)	111.13(3)
Cu(8)-Cu(12)-Cu(9)	59.17(3)
Cu(7)-Cu(12)-Cu(9)	102.62(3)
Cu(11)-Cu(12)-Cu(9)	89.08(3)
Cu(3)-S(1)-Cu(1)	129.21(4)
Cu(3)-S(1)-Cu(2)	78.48(5)
Cu(1)-S(1)-Cu(2)	77.99(4)
Cu(3)-S(1)-Cu(4)	82.26(4)
Cu(1)-S(1)-Cu(4)	79.31(4)
Cu(2)-S(1)-Cu(4)	129.65(5)
Cu(5)-S(2)-Cu(8)	85.91(4)
Cu(5)-S(2)-Cu(9)	68.82(4)
Cu(8)-S(2)-Cu(9)	73.75(4)
Cu(5)-S(2)-Cu(1)	72.40(4)
Cu(8)-S(2)-Cu(1)	69.82(3)
Cu(9)-S(2)-Cu(1)	127.75(4)
Cu(5)-S(3)-Cu(6)	85.32(4)
Cu(5)-S(3)-Cu(10)	72.53(3)
Cu(6)-S(3)-Cu(10)	69.48(4)
Cu(5)-S(3)-Cu(2)	69.48(4)

Cu(6)-S(3)-Cu(2)	72.66(4)
Cu(10)-S(3)-Cu(2)	127.57(5)
Cu(6)-S(4)-Cu(7)	84.83(4)
Cu(6)-S(4)-Cu(3)	69.31(3)
Cu(7)-S(4)-Cu(3)	73.73(4)
Cu(6)-S(4)-Cu(11)	72.92(3)
Cu(7)-S(4)-Cu(11)	69.58(3)
Cu(3)-S(4)-Cu(11)	128.78(4)
Cu(7)-S(5)-Cu(8)	84.87(4)
Cu(7)-S(5)-Cu(4)	69.79(3)
Cu(8)-S(5)-Cu(4)	73.03(4)
Cu(7)-S(5)-Cu(12)	74.08(4)
Cu(8)-S(5)-Cu(12)	69.01(3)
Cu(4)-S(5)-Cu(12)	129.03(5)
Cu(10)-S(6)-Cu(11)	80.23(4)
Cu(10)-S(6)-Cu(12)	128.92(5)
Cu(11)-S(6)-Cu(12)	79.75(4)
Cu(10)-S(6)-Cu(9)	76.91(4)
Cu(11)-S(6)-Cu(9)	128.62(4)
Cu(12)-S(6)-Cu(9)	80.05(5)

Table S4. Lowest excitation energies for $[Cu_{12}S_6(dpppt)_4]$ (**1**) and $[Cu_{12}S_6(dppo)_4]$ (**2**) obtained at different levels of theory. Molecule **1** is of C_i symmetry, dipole-allowed (representation a_u) and dipole-forbidden (a_g) transitions are listed separately. Additionally to the excitation energy E (in eV) the dominant orbital contributions are listed, column 'char'. Herein, H denotes the HOMO, H–1 the HOMO–1, etc. Besides 'conventional' treatments like singlet and triplet excitations with B3LYP (B3-LYP/S→S and B3-LYP/S→T) and singlet excitations with BP86 (BP86/S→S) also results for spinflip TDDFT[15] with LDA[16] for the direct calculation of the triplet-singlet de-excitation (SF-PWLDA/T→S) are listed. The latter method uses the self-consistently calculated lowest excited triplet state as reference.

Method/transition	**1**				**2**	
	dipole-allowed		dipole-forbidden			
	E	char	*E*	char	*E*	char
B3-LYP/S→S	2.57	(H–1)→L	2.47	H→L	2.33	H→L
B3-LYP/S→T	2.54	(H–1)→L	2.43	H→L	2.35	H→L
BP86/S→S	1.66	H→(L+1)	1.58	H→L	1.49	H→L
SF-PWLDA/T→S	1.85		1.69		1.54	

Table S5. Lowest 60 singlet and triplet transitions for $[Cu_{12}S_6(dpppt)_4]$ (**1**) and $[Cu_{12}S_6(dppo)_4]$ (**2**) at level B3LYP/def2-SV(P) (raw data for figure S10). Excitation energies, *E*, in eV, oscillator strengths *f* are given in the mixed representation.

1				**2**			
Singlet excitations		Triplet excitations		Singlet excitations		Triplet excitations	
E	*f*	*E*	*f*	*E*	*f*	*E*	*f*
2.4656	0.00E-00	2.4293	0.00E-00	2.3290	0.17E-02	2.3475	0.42E-02
2.5707	0.22E-02	2.5384	0.14E-01	2.4017	0.82E-05	2.4269	0.89E-04
2.6566	0.00E-00	2.6096	0.00E-00	2.4952	0.89E-02	2.4836	0.60E-01
2.7075	0.00E-00	2.6350	0.10E-00	2.5187	0.10E-01	2.5195	0.51E-01
2.7392	0.62E-02	2.6481	0.53E-01	2.5537	0.48E-02	2.5460	0.13E-02
2.7581	0.11E-01	2.6600	0.00E-00	2.6201	0.10E-01	2.5866	0.35E-01
2.7853	0.10E-01	2.7428	0.50E-01	2.6272	0.25E-03	2.6497	0.27E-03
2.7925	0.00E-00	2.7469	0.00E-00	2.8585	0.38E-02	2.8599	0.10E-01
2.8154	0.00E-00	2.7932	0.00E-00	2.8907	0.29E-02	2.8890	0.64E-02
2.8213	0.00E-00	2.7941	0.00E-00	2.9132	0.20E-02	2.9164	0.22E-02
2.8282	0.60E-02	2.7974	0.25E-01	2.9159	0.30E-02	2.9197	0.82E-02
2.8931	0.00E-00	2.8584	0.00E-00	2.9411	0.38E-03	2.9463	0.10E-02
2.8935	0.91E-02	2.8603	0.58E-01	2.9706	0.85E-03	2.9758	0.17E-02
2.8993	0.00E-00	2.8761	0.42E-01	2.9786	0.14E-02	2.9832	0.26E-02
2.9042	0.62E-02	2.8867	0.00E-00	2.9830	0.55E-03	2.9884	0.40E-03
2.9151	0.32E-03	2.9050	0.56E-03	3.0033	0.74E-03	3.0105	0.25E-02
2.9278	0.00E-00	2.9132	0.00E-00	3.0097	0.19E-02	3.0163	0.46E-02
2.9311	0.31E-02	2.9257	0.20E-01	3.0244	0.12E-02	3.0279	0.53E-02
2.9573	0.00E-00	2.9288	0.00E-00	3.0264	0.52E-03	3.0332	0.79E-03
2.9614	0.30E-02	2.9451	0.27E-01	3.0344	0.51E-02	3.0418	0.79E-02
2.9763	0.00E-00	2.9611	0.00E-00	3.0504	0.17E-03	3.0609	0.12E-03
2.9876	0.17E-02	2.9697	0.30E-02	3.0537	0.29E-03	3.0621	0.17E-02
2.9977	0.00E-00	2.9801	0.00E-00	3.0562	0.55E-03	3.0706	0.70E-03
3.0039	0.70E-02	2.9850	0.40E-01	3.0644	0.20E-03	3.0845	0.91E-03
3.0063	0.00E-00	2.9911	0.00E-00	3.0895	0.60E-02	3.0968	0.80E-02
3.0135	0.00E-00	3.0019	0.00E-00	3.0906	0.36E-02	3.0986	0.49E-02
3.0218	0.88E-02	3.0049	0.85E-02	3.0978	0.10E-02	3.1150	0.17E-02
3.0254	0.14E-02	3.0172	0.22E-01	3.1112	0.84E-03	3.1173	0.17E-02
3.0313	0.00E-00	3.0176	0.00E-00	3.1129	0.75E-03	3.1203	0.68E-03
3.0530	0.11E-01	3.0272	0.13E-00	3.1190	0.38E-02	3.1264	0.33E-02
3.0547	0.00E-00	3.0401	0.00E-00	3.1217	0.18E-02	3.1320	0.52E-02
3.0682	0.00E-00	3.0417	0.71E-01	3.1287	0.14E-02	3.1368	0.39E-02
3.0692	0.66E-02	3.0510	0.00E-00	3.1397	0.95E-03	3.1543	0.10E-02
3.0748	0.00E-00	3.0559	0.00E-00	3.1481	0.19E-02	3.1620	0.51E-03
3.0821	0.39E-02	3.0691	0.17E-01	3.1570	0.37E-03	3.1680	0.22E-02
3.0859	0.00E-00	3.0734	0.35E-01	3.1600	0.26E-02	3.1691	0.10E-02
3.0921	0.71E-03	3.0709	0.00E-00	3.1628	0.16E-02	3.1742	0.31E-02
3.0990	0.71E-02	3.0826	0.00E-00	3.1836	0.38E-02	3.1940	0.11E-02
3.0993	0.00E-00	3.0854	0.36E-01	3.1945	0.53E-03	3.2024	0.36E-04
3.1011	0.00E-00	3.0889	0.00E-00	3.1986	0.28E-02	3.2106	0.19E-02
3.1070	0.73E-03	3.0935	0.15E-01	3.2011	0.20E-02	3.2122	0.42E-02
3.1219	0.00E-00	3.0978	0.92E-01	3.2064	0.34E-02	3.2177	0.38E-02
3.1228	0.12E-01	3.1019	0.00E-00	3.2138	0.49E-02	3.2244	0.41E-02
3.1283	0.00E-00	3.1060	0.11E-01	3.2225	0.20E-02	3.2333	0.33E-03
3.1293	0.24E-02	3.1145	0.00E-00	3.2260	0.40E-02	3.2358	0.60E-02
3.1363	0.15E-02	3.1255	0.14E-02	3.2307	0.85E-03	3.2486	0.35E-02
3.1481	0.00E-00	3.1258	0.00E-00	3.2425	0.47E-02	3.2551	0.92E-02
3.1523	0.62E-02	3.1392	0.14E-01	3.2485	0.51E-02	3.2609	0.54E-02
3.1566	0.00E-00	3.1394	0.00E-00	3.2523	0.47E-02	3.2630	0.23E-02
3.1653	0.12E-02	3.1431	0.24E-01	3.2540	0.40E-04	3.2640	0.10E-02
3.1680	0.00E-00	3.1512	0.00E-00	3.2578	0.27E-02	3.2673	0.15E-02
3.1755	0.56E-02	3.1522	0.90E-02	3.2625	0.87E-03	3.2774	0.24E-02
3.1765	0.26E-02	3.1576	0.00E-00	3.2788	0.14E-02	3.2915	0.30E-02
3.1774	0.00E-00	3.1634	0.14E-01	3.2874	0.30E-02	3.3001	0.11E-02
3.1831	0.16E-02	3.1671	0.44E-01	3.2903	0.16E-02	3.3034	0.77E-02
3.1846	0.00E-00	3.1677	0.00E-00	3.2994	0.32E-02	3.3135	0.19E-02
3.1918	0.81E-02	3.1714	0.00E-00	3.3066	0.19E-02	3.3213	0.32E-02
3.1948	0.00E-00	3.1715	0.58E-01	3.3106	0.18E-01	3.3272	0.14E-01
3.2059	0.97E-02	3.1772	0.51E-01	3.3146	0.25E-02	3.3303	0.50E-03
3.2084	0.00E-00	3.1871	0.00E-00	3.3202	0.15E-02	3.3446	0.28E-02

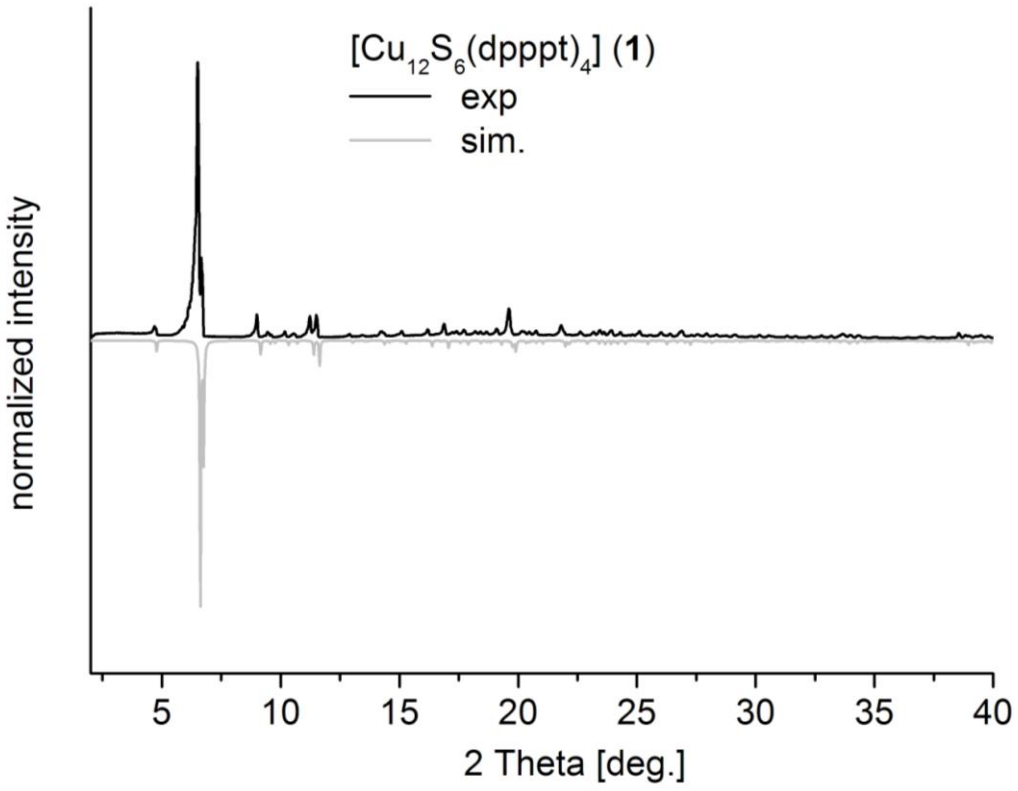

Figure S1. Measured (black) and simulated (grey) X–ray powder pattern for $[Cu_{12}S_6(dpppt)_4]$ (**1**) as a suspension of crystals in toluene.

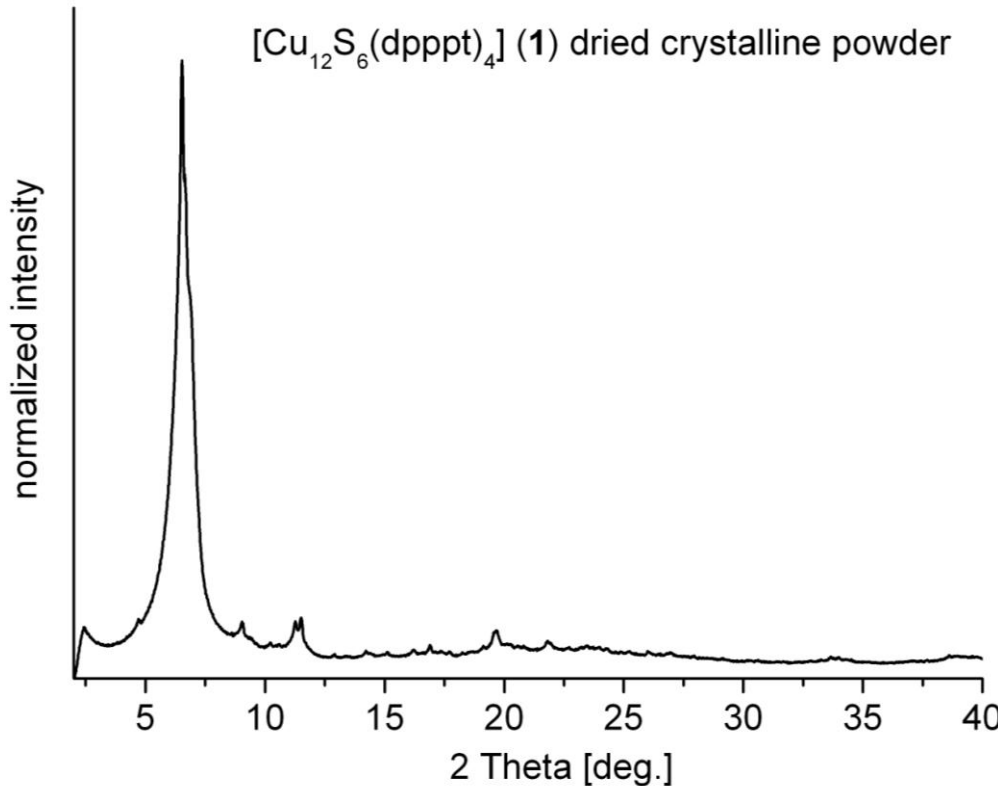

Figure S2. X–ray powder pattern for $[Cu_{12}S_6(dpppt)_4]$ (**1**) as a dried crystalline powder.

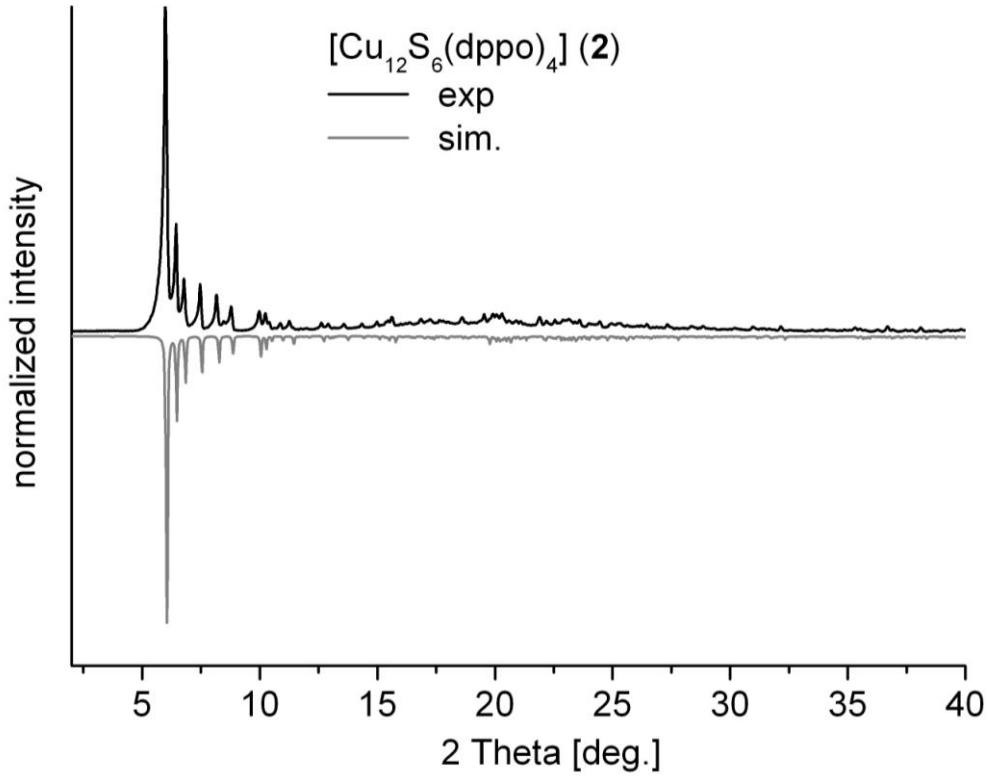

Figure S3. Measured (black) and simulated (grey) X–ray powder pattern for $[Cu_{12}S_6(dppo)_4]$ (**2**) as a suspension of crystals in toluene.

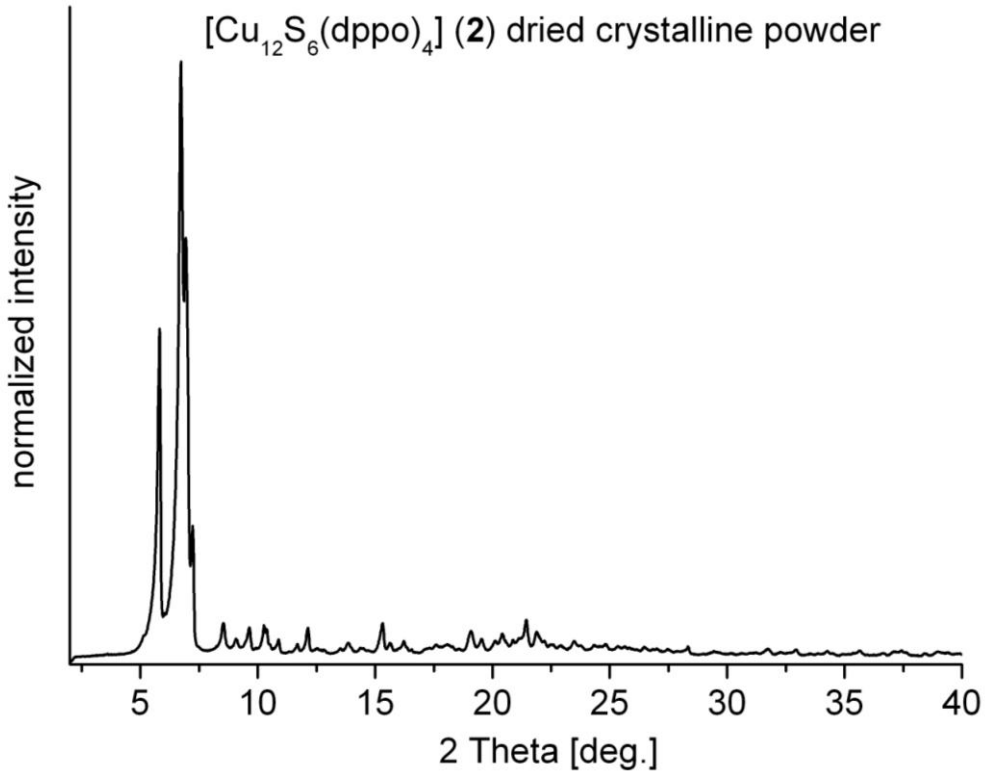

Figure S4. X–ray powder pattern of $[Cu_{12}S_6(dppo)_4]$ (**2**) as a dried crystalline powder.

a)

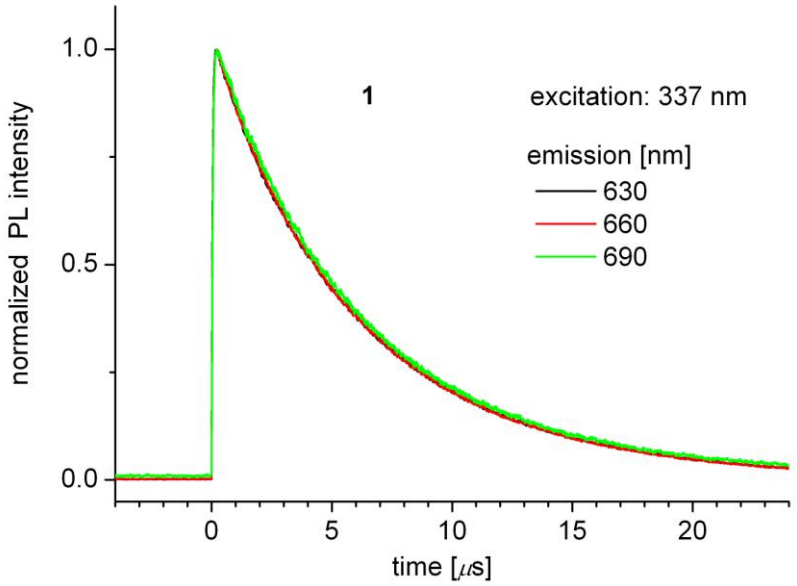

b)

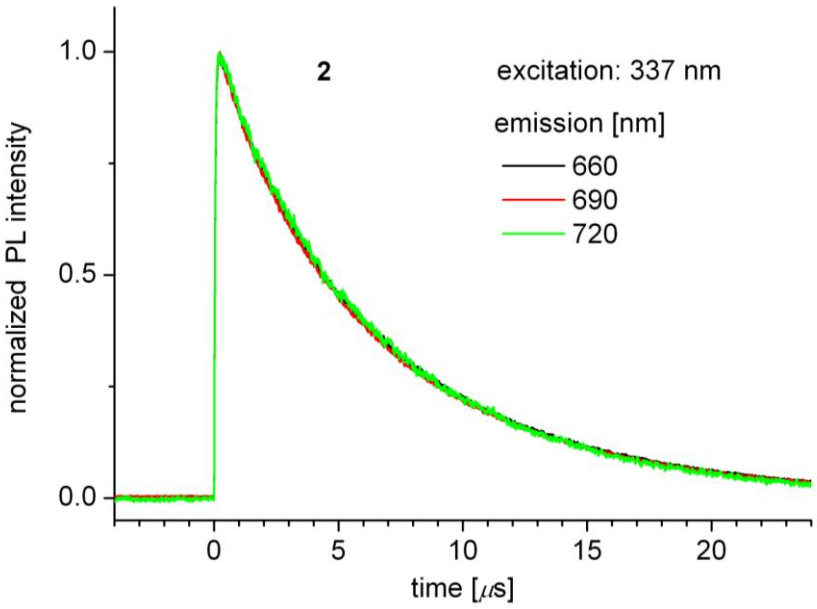

Figure S5. Emission decay traces under 337 nm pulse excitation for a) $[Cu_{12}S_6(dpppt)_4]$ (**1**) and b) $[Cu_{12}S_6(dppo)_4]$ (**2**) as a suspension of microcrystals in toluene. The measurements were performed at ambient temperature (295 K).

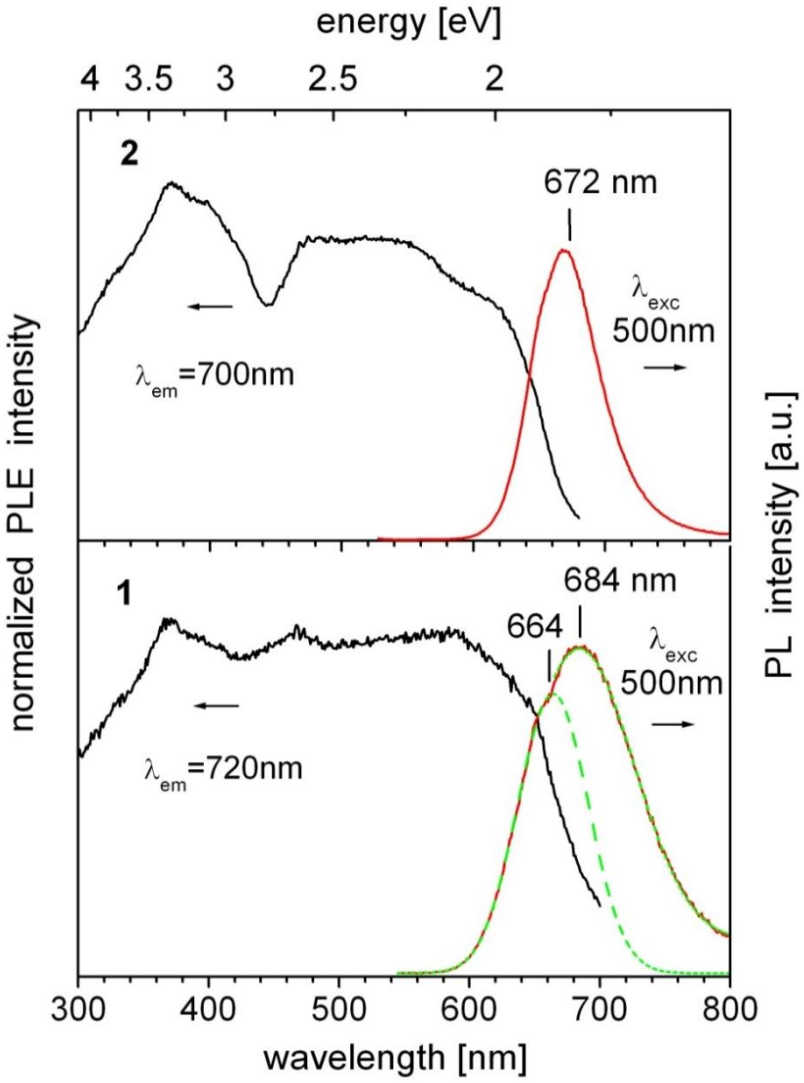

Figure S6. Steady-state photoluminescence excitation and emission spectra for $[Cu_{12}S_6(dpppt)_4]$ (**1**) (down) and $[Cu_{12}S_6(dppo)_4]$ (**2**) (up) as dried crystalline powders measured in an integrating sphere at ambient temperature. Green dotted lines represent fits by a Gauss function.

a)

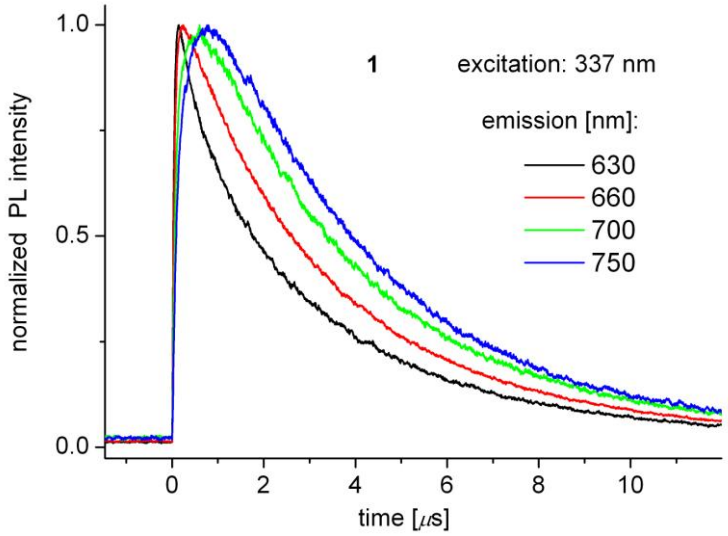

b)

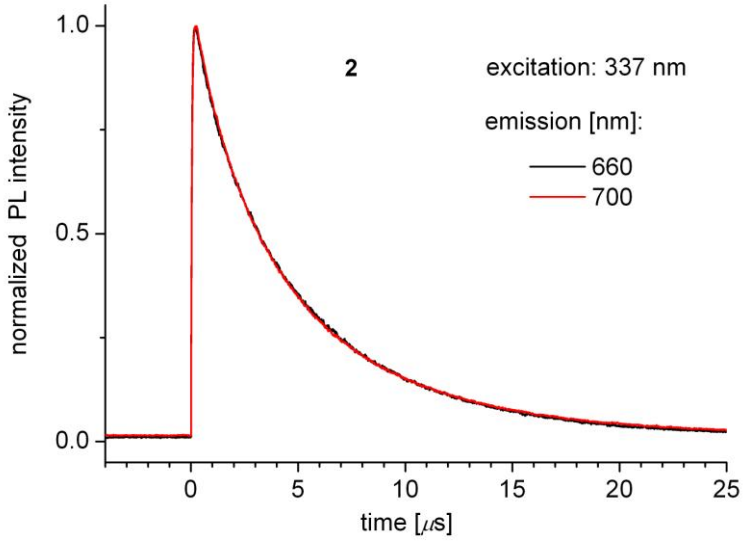

Figure S7. Photoluminescence decay traces for a) $[Cu_{12}S_6(dpppt)_4]$ (**1**) and b) $[Cu_{12}S_6(dppo)_4]$ (**2**) as dried crystalline powders excited at 337 nm (N_2-laser) at ambient temperature.

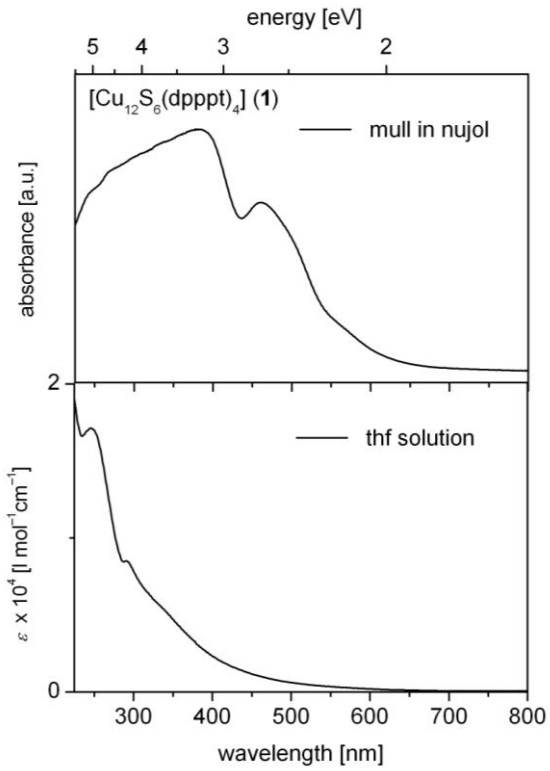

Figure S8. UV-Vis spectra of $[Cu_{12}S_6(dpppt)_4]$ (**1**) as a mull of a crystalline powder in nujol (up) and as a solution in thf (down).

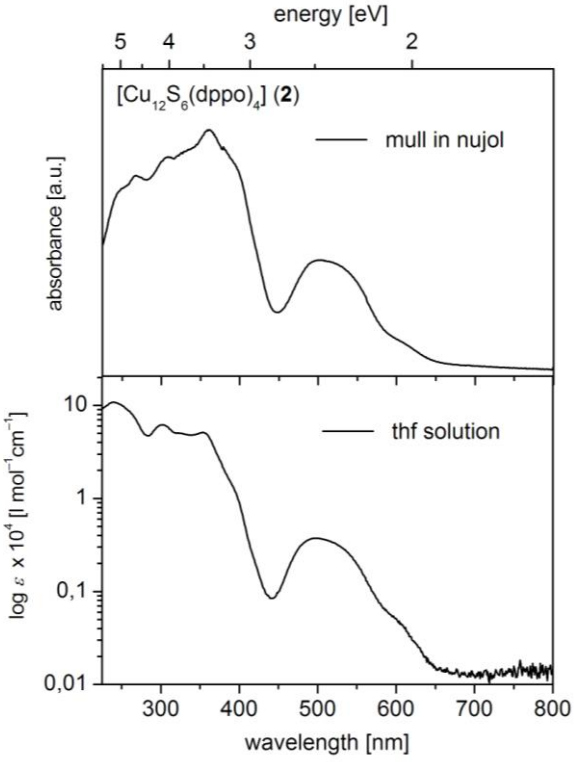

Figure S9. UV-Vis spectra of $[Cu_{12}S_6(dppo)_4]$ (**2**) as a mull of a crystalline powder in nujol (up) and as a solution in thf (down).

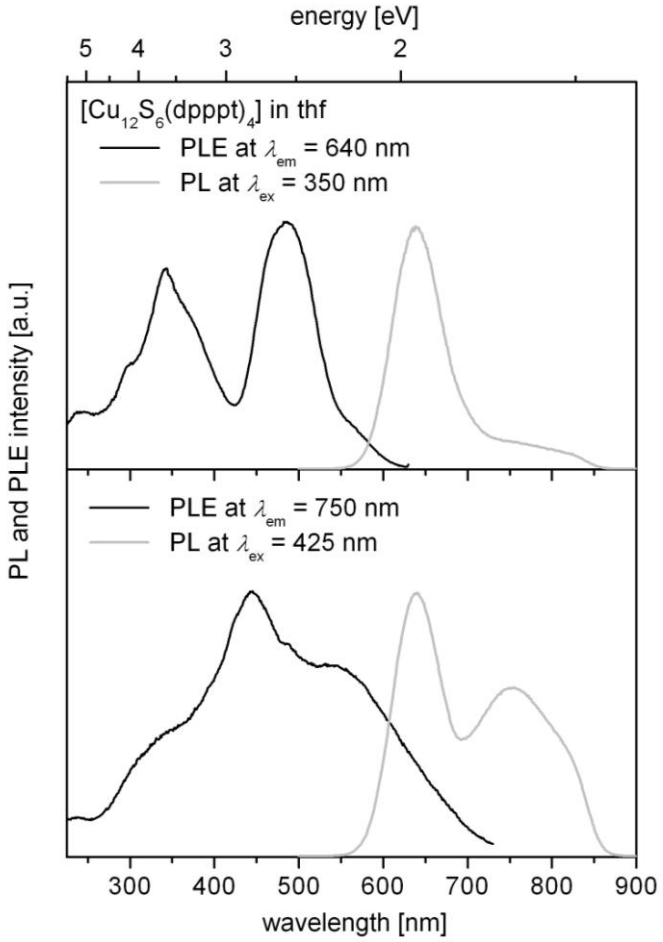

Figure S10. PLE and PL spectra of $[Cu_{12}S_6(dpppt)_4]$ (**1**) in thf.

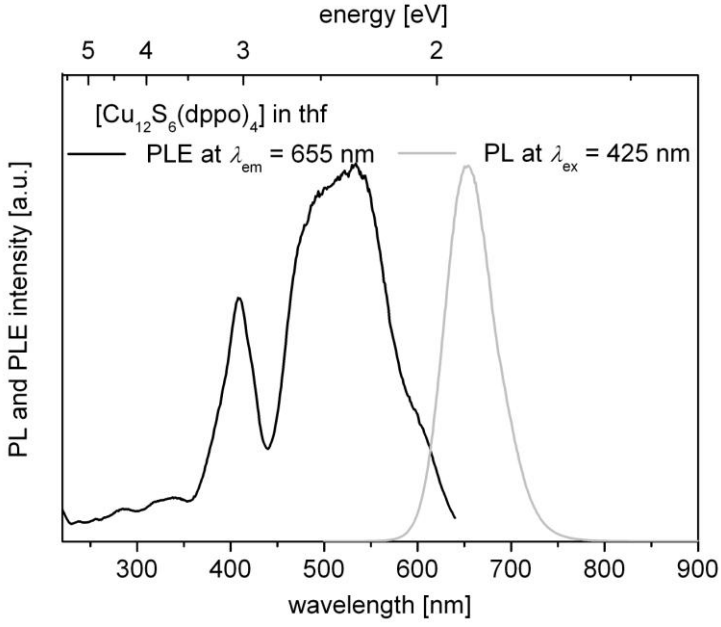

Figure S11. PLE and PL spectra of $[Cu_{12}S_6(dppo)_4]$ (**2**) in thf.

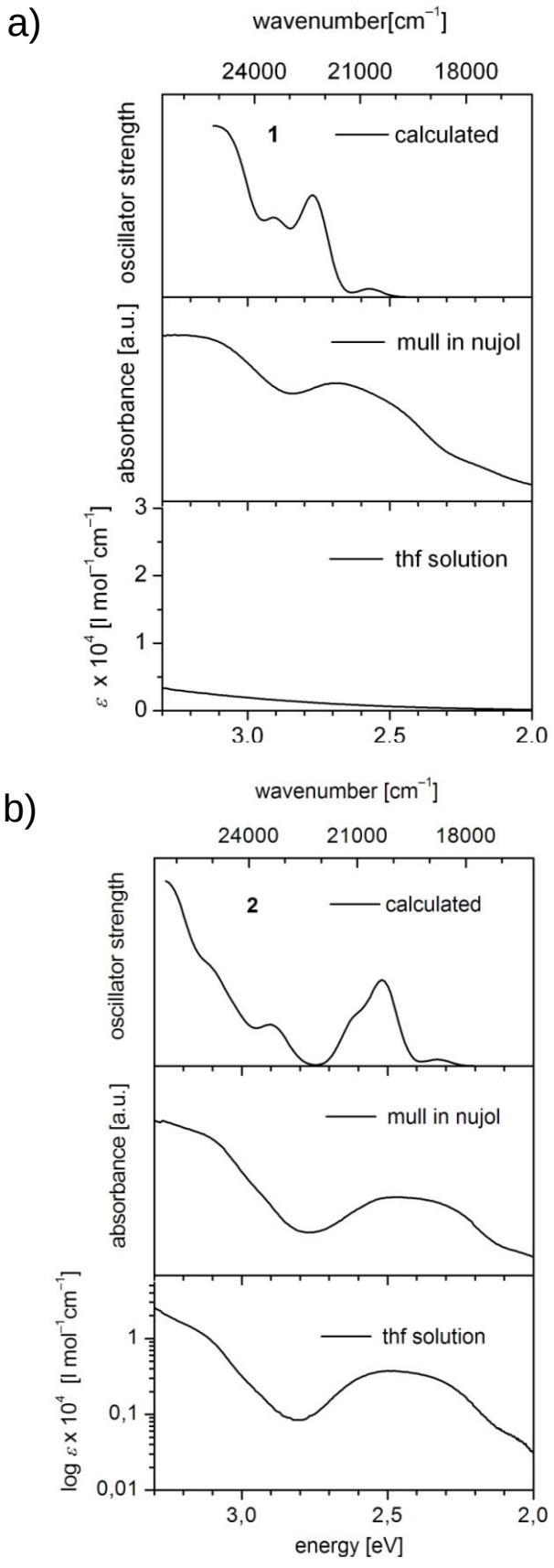

Figure S12. Comparison of calculated excitation spectra (at level B3-LYP/def2-SV(P), see also Figure 3) of a) $[Cu_{12}S_6(dpppt)_4]$ (**1**) and b) $[Cu_{12}S_6(dppo)_4]$ (**2**) with the experimental absorption spectra as a mull of a crystalline powder in nujol and as a solution in thf.

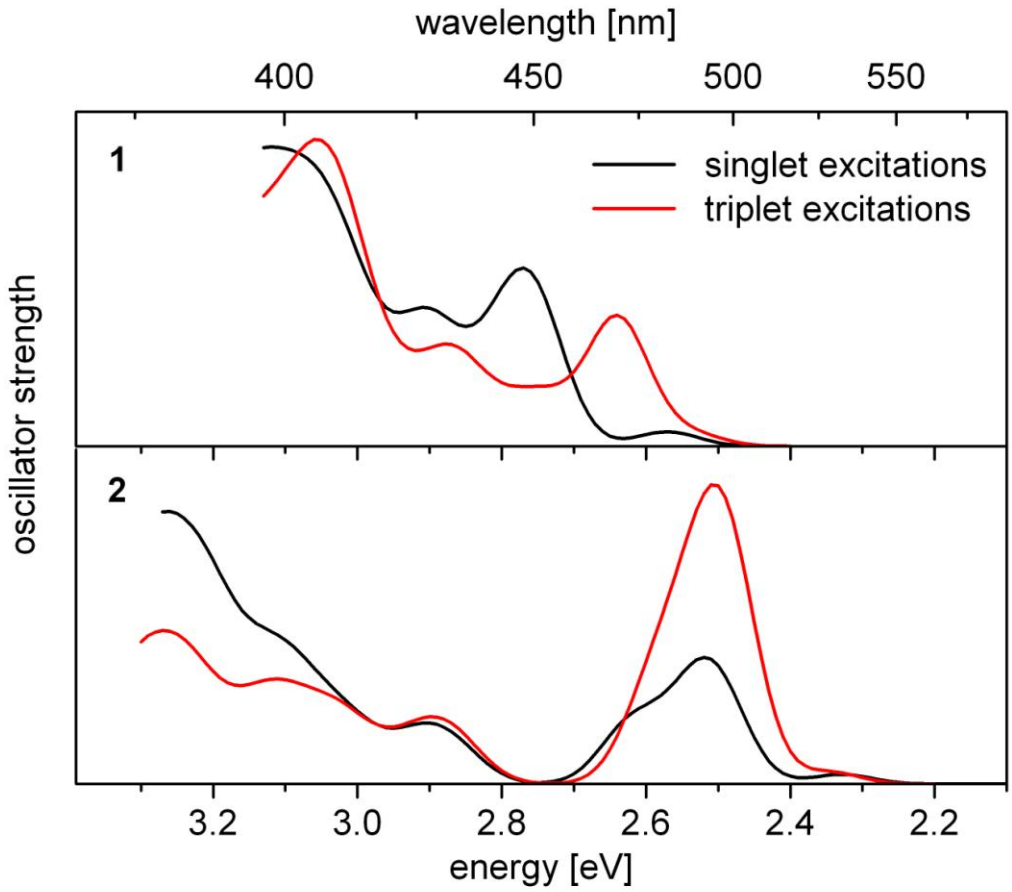

Figure S13. Calculated electronic singlet (black) and triplet (red) excitation spectra (lowest 60 singlet excitations, superimposed Gaussians of FWHM=0.1eV for each transition) for the X-ray structure of $[Cu_{12}S_6(dpppt)_4]$ (**1**) and $[Cu_{12}S_6(dppo)_4]$ (**2**) at level B3-LYP/def2-SV(P). Note, that oscillator strengths have in the case of the calculated triplet spectra no physical meaning.

a)

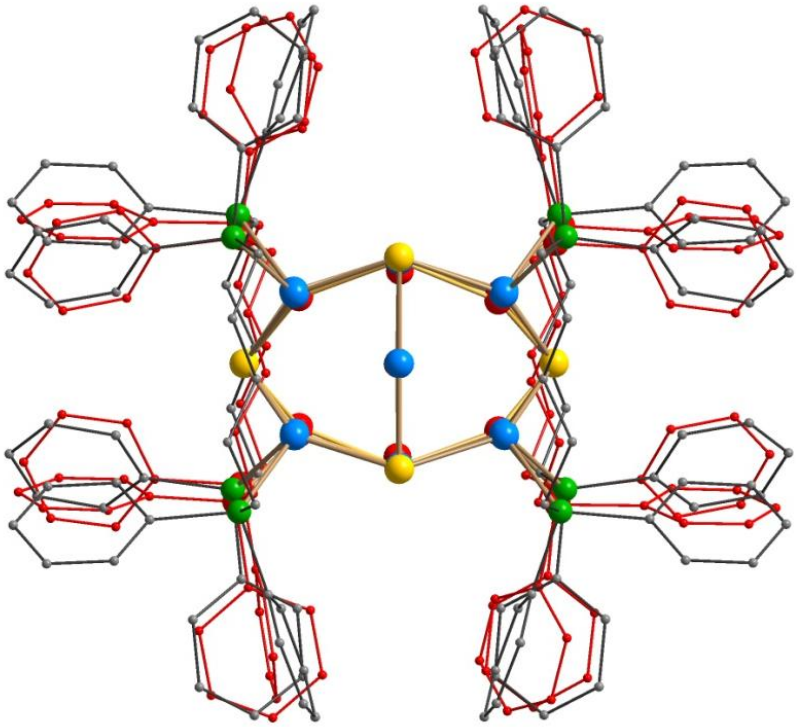

b)

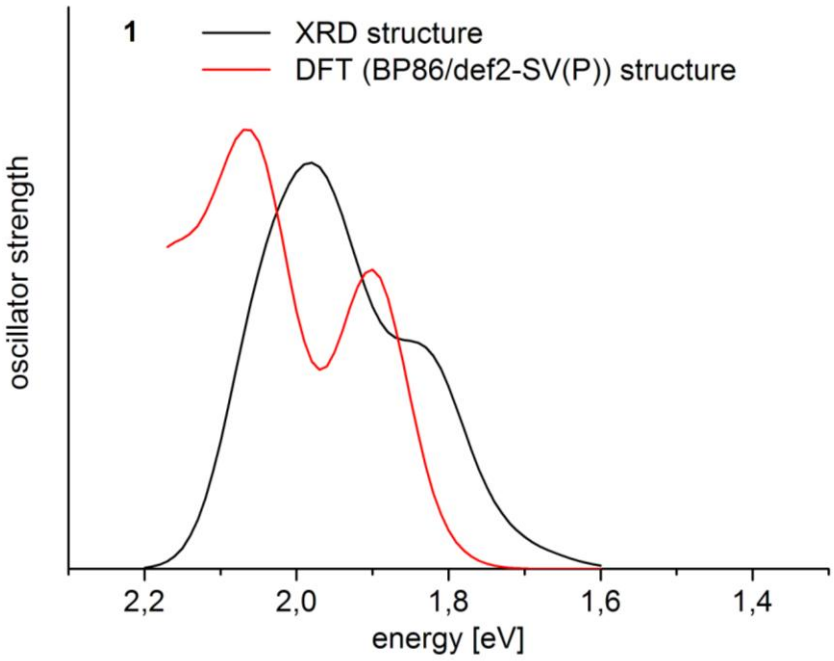

Figure S14. a) Comparison of the molecular structures of $[Cu_{12}S_6(dpppt)_4]$ (**1**) as obtained from single crystal XRD (in front; Cu: blue, S: yellow, P. green, C: grey) and as optimized with DFT(BP86/def2-SV(P)) (in the back; all atoms red) and b) Calculated electronic excitation spectra at level BP86/def2-SV(P) (lowest energy singlet excitations, superimposed Gaussians of FWHM=0.1eV for each transition) for the experimental structure of **1** obtained by single crystal X-ray diffraction (black) and the corresponding ground state structure optimized with DFT (red).

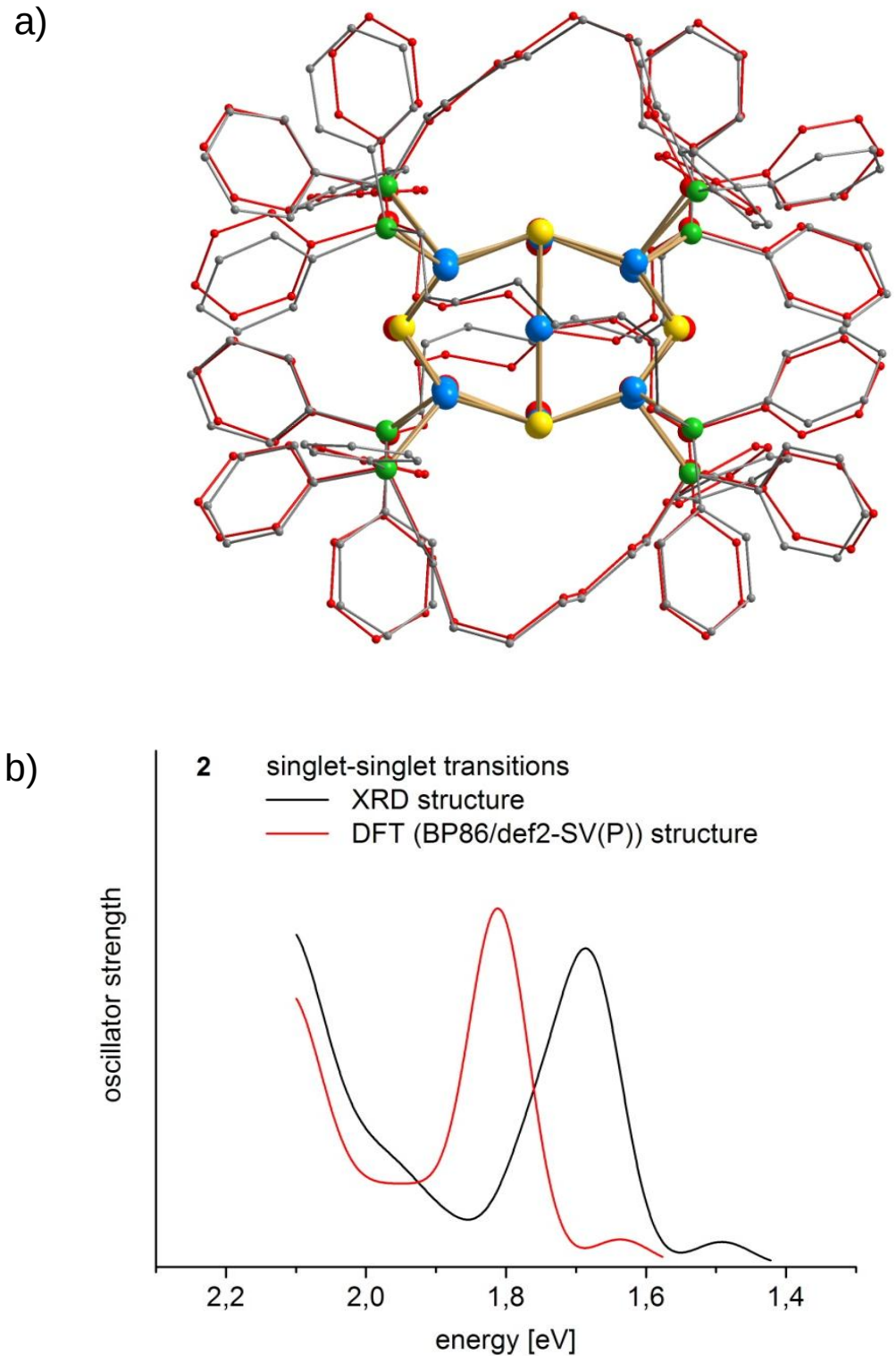

Figure S15. a) Comparison of the molecular structures of $[Cu_{12}S_6(dppo)_4]$ (**2**) as obtained from single crystal XRD (in front; Cu: blue, S: yellow, P. green, C: grey) and as optimized with DFT(BP86/def2-SV(P) (in the back; all atoms red) and b) Calculated electronic excitation spectra at level BP86/def2-SV(P) (lowest energy singlet excitations, superimposed Gaussians of FWHM=0.1eV for each transition) for the experimental structure of **2** obtained by single crystal X-ray diffraction (black) and the corresponding ground state structure optimized with DFT (red).

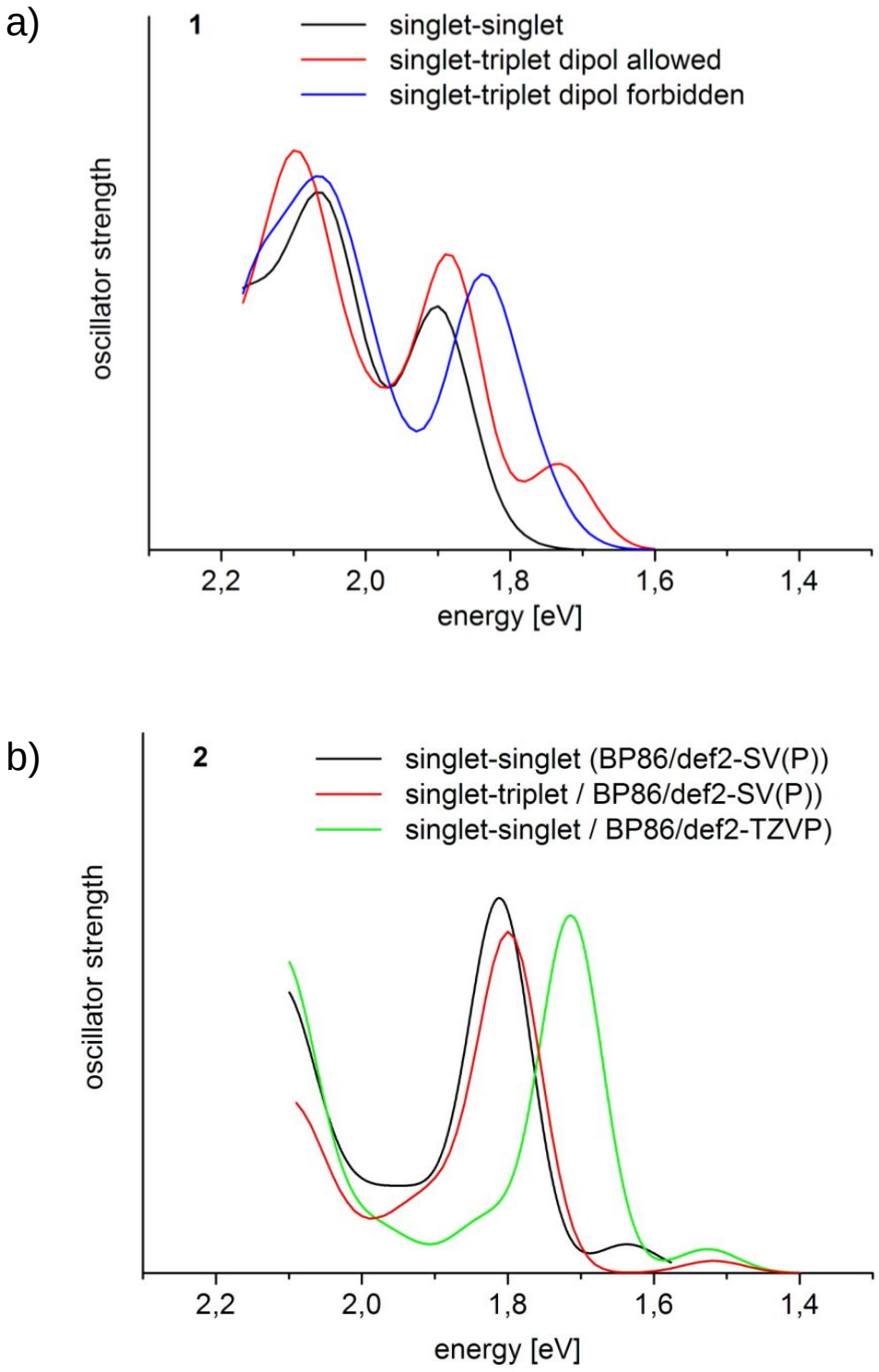

Figure S16. Comparison of calculated electronic singlet (black) and triplet (red and blue) excitation spectra at level BP86/def2-SV(P) (lowest energy excitations, superimposed Gaussians of FWHM=0.1eV for each transition) for DFT-optimized (BP86/def2-SV(P)) structure parameters of the molecular structures of a) $[Cu_{12}S_6(dpppt)_4]$ (**1**) and b) $[Cu_{12}S_6(dppo)_4]$ (**2**). For **2** singlet excitation spectra were also calculated for two different basis sets namely def2-SV(P) (black) and def2-TZVP (green). Note, that oscillator strengths have in the case of the calculated triplet spectra no physical meaning.

References

(1) D. A. Edwards, R. Richards, *J. Chem. Soc. Dalton Trans*. **1973**, 2463-2468.

(2) H. Schmidt, H. Ruf, *Z. Anorg. Allg. Chem.***1963**, *321*, 270-273.

(3) X-RED32 1.01, Data Reduction Program, STOE&CIE GmbH, Darmstadt, Germany, 2001.

(4) G. M. Sheldrick, SHELXTL PC version 5.1 An Integrated System for Solving, Refining, and Displaying Crystal Structures from Diffraction Data, Bruker Analytical X-ray Systems, Karlsruhe, **2000**.

(5) Diamond Version 2.1d, K. Brandenburg, Crystal Impact GbR, **1996-2000**.

(6) A.L. Spek, *Acta Cryst*. **1990**, A*46*, C-34.

(7) STOE, WinXPOW, STOE &Cie GmbH, Darmstadt, **2000**.

(8) S. Lebedkin, T. Langetepe, P. Sevillano, D. Fenske, M. M. Kappes, *J. Phys. Chem. B* **2002**, *106*, 9019-9026.

(9) R. F. Kubin, A. N. Fletcher, *J. Luminesc.* **1983**, *27*, 455–462.

(10) TURBOMOLE Version 6.5, TURBOMOLE GmbH 2013. TURBOMOLE is a development of University of Karlsruhe and Forschungszentrum Karlsruhe 1989-2007, TURBOMOLE GmbH since 2007.

(11) a) C. Lee, W. Yang, R. G. Parr, *Phys. Rev. B*, **1988**, *37*, 785-789; b) A. D. Becke, *J. Chem. Phys.* **1993**, *98*, 5648-5652.

(12) F. Weigend, R. Ahlrichs, *Phys. Chem. Chem. Phys.* **2005**, *7*, 3297-3305.

(13) L. Laaksonen, *J. Mol. Graph.* **1992,** *10***,** 33-34.

(14) A. D. Becke, *Phys Rev. A* **1988,** *38*, 3098-3100; b) J. P. Perdew, *Phys. Rev. B* **1986**, *33*, 8822-8824.

(15) M. Kühn, F. Weigend, *ChemPhysChem*, **2011**, *12*, 3331-3336.

(16) J. P. Perdew, Y. Wang, *Phys. Rev. B*, **1992**, *45*, 13244-13249.